quantified 5–7 d after transfection of cells with RNA interference (RNAi) duplexes using the CellTiter-Glo Luminescent Cell Viability Assay (Promega), a luminescence-based method to determine the number of viable cells.

For rescue of the *RHOA* knockdown phenotype, SW948 cells expressing siRNA-resistant wild-type and mutant *RHOA* were prepared. *RHOA* siRNAs 2 and 3 recognize the 3′ UTR of *RHOA*, so we introduced the coding sequence of *RHOA* as for siRNA-resistant wild-type and mutant *RHOA* constructs. The coding sequence for *RHOA* was amplified by RT-PCR from AGS cells and inserted into the pEBMulti-Neo vector (Wako). Expression plasmids for Gly17Glu and Tyr42Cys mutant RHOA were generated using site-directed-mutagenesis PCR and the In-Fusion HD Cloning system (Clontech) with plasmid encoding wild-type RHOA. Each plasmid was transfected into SW948 cells by electroporation with the Nucleofector system (Lonza). Cell growth inhibition assays were performed with transfected cells transiently expressing siRNA-resistant wild-type and mutant RHOA.

Quantitative RT-PCR and protein blot analyses. Cells were seeded in 6-well ultra-low-attachment plates (Corning) at a density of 2.5×10^5 cells per well. At the same time, mixtures of siRNA and Lipofectamine RNAiMAX reagent were added to each well as 0.2 or 1 nM siRNA solutions. Two days after transfection, total RNA was extracted using the RNeasy Mini kit (Qiagen). Quantitative RT-PCR was performed with Power SYBR Green PCR Master Mix (Applied Biosystems), using primers for *RHOA* or *RPS18* (primer sequences are listed in **Supplementary Table 6**). Values obtained in quantitative RT-PCR were normalized to those for *RPS18*.

Two days after transfection, cells were also lysed in RIPA buffer (188-02453, Wako) supplemented with a protease inhibitor cocktail (4693132, Roche) and the phosphatase inhibitor PhosSTOP (4906845, Roche), and concentrations for the extracts ware estimated with the DC protein assay (Bio-Rad). Total cell extract (5 μg of protein per lane) was subjected to protein blot analyses. Blotted membranes were probed with rabbit monoclonal antibody to RHOA (2117, Cell Signaling Technology) and with mouse monoclonal antibody to β-actin (A1978, Sigma-Aldrich). Antibodies were diluted by 1:1,000 (RHOA) and 1:4,000 (β-actin).

Structural analysis. The structural model was generated from PDB 1X86, using Discovery Studio (Accelrys) and PyMol (Schrodinger). The Tyr42 and Gly17 residues in RHOA are shown by stick model (magenta, carbon; red, oxygen; blue, nitrogen). GDP is shown by stick model (yellow, carbon; red, oxygen; blue, nitrogen; orange, phosphorus).

32. Li, H. & Durbin, R. Fast and accurate short read alignment with Burrows-Wheeler transform. *Bioinformatics* **25**, 1754–1760 (2009).
33. Homer, N. & Nelson, S.F. Improved variant discovery through local re-alignment of short-read next-generation sequencing data using SRMA. *Genome Biol.* **11**, R99 (2010).
34. Song, S. *et al.* qpure: A tool to estimate tumor cellularity from genome-wide single-nucleotide polymorphism profiles. *PLoS ONE* **7**, e45835 (2012).
35. Carter, S.L. *et al.* Absolute quantification of somatic DNA alterations in human cancer. *Nat. Biotechnol.* **30**, 413–421 (2012).
36. Wang, K., Li, M. & Hakonarson, H. ANNOVAR: functional annotation of genetic variants from high-throughput sequencing data. *Nucleic Acids Res.* **38**, e164 (2010).
37. Qin, J., Jones, R.C. & Ramakrishnan, R. Studying copy number variations using a nanofluidic platform. *Nucleic Acids Res.* **36**, e116 (2008).
38. Dube, S., Qin, J. & Ramakrishnan, R. Mathematical analysis of copy number variation in a DNA sample using digital PCR on a nanofluidic device. *PLoS ONE* **3**, e2876 (2008).

STEM CELLS®

EMBRYONIC STEM CELLS/INDUCED PLURIPOTENT STEM CELLS

Knockdown of Nucleosome Assembly Protein 1-Like 1 Induces Mesoderm Formation and Cardiomyogenesis Via Notch Signaling in Murine-Induced Pluripotent Stem Cells

HUI GONG,[a] YUAN YAN,[a] BO FANG,[a] YUANYUAN XUE,[a] PEIPEI YIN,[a] LU LI,[a] GUOPING ZHANG,[a] XIA SUN,[a] ZHIDAN CHEN,[a] HONG MA,[b] CHUNJIE YANG,[a] YINGJIONG DING,[c] YE YONG,[a] YICHUN ZHU,[c] HUANGTIAN YANG,[d] ISSEI KOMURO,[e] JUNBO GE,[a] YUNZENG ZOU[a]

Key Words. Nap1l1 • Induced pluripotent stem cells • Cardiomyocyte • Cardiac differentiation

ABSTRACT

Low efficiency of cardiomyocyte differentiation from induced pluripotent stem cells (iPSCs) hinders the clinical application of iPSC technology for cardiac repair strategy. Recently, we screened out nucleosome assembly protein 1-like 1 (Nap1l1), which was downregulated during the differentiation of P19CL6 cells into cardiomyocytes. Here, we attempted to study the role of Nap1l1 in cardiomyogenesis of iPSC. Nap1l1 was downregulated during the differentiation of iPSC. Knockdown of Nap1l1 dramatically enhanced the differentiation of iPSC into functional cardiomyocytes while overexpression of Nap1l1 sharply lowered the differentiation. Moreover, although Nap1l1-knockdown had little effect on endoderm differentiation, the Nap1l1 modulation significantly accelerated mesoderm development. Re-expressing Nap1l1 in Nap1l1-knockdown-iPSC rescued the effects of Nap1l1. Inducibly overexpressing Nap1l1 at early stage of differentiation greatly inhibited mesoderm induction and cardiogenesis of iPSC. However, mesoderm stem cells (Flk-1-positive cells) originated from Nap1l1-knockdown- or -overexpression-iPSC showed no difference in further cardiomyocyte differentiation compared with that of control-iPSC. Further study revealed that Nap1l1-overexpression increased γ-secretase activity and the expression of Notch intracellular domain (NICD) and downstream genes during the differentiation of iPSC. γ-Secretase inhibitor DAPT (N-[N-(3,5-difluorophenacetyl)-L-alanyl]-S-phenylglycinet-butyl ester) greatly suppressed the production of NICD and abolished the inhibitory effects of Nap1l1-overexpression on mesoderm induction and cardiogenesis. These findings demonstrate that downregulation of Nap1l1 significantly enhances mesodermal induction and subsequent cardiogenesis of murine iPSC via inhibition of γ-secretase-regulated Notch signaling, which would facilitate the application of iPSC in heart diseases. STEM CELLS *2014;32:1759–1773*

INTRODUCTION

During myocardial infarction, irreversible cardiomyocytes loss may lead to the development of progressive heart failure [1]. Cell therapy is an emerging technology to repopulate the injured heart and improve cardiac function of the failing heart. The development of induced pluripotent stem cells (iPSCs) has opened up new opportunities for basic research and regenerative medicine [2, 3]. Cardiomyocytes from mouse and human iPSC have similar characteristics to those derived from authentic mouse and human embryonic stem cells (ESC) [4, 5]. Thus, iPSC could be an alternative source of functionally intact cardiomyocytes for cardiovascular diseases treatment. However, this promising approach has been hampered mainly due to limited generation of functional cardiomyocytes from iPSC.

We sought to identify novel factors that may efficiently promote differentiation of iPSC into functional cardiomyocytes in the differentiation system. In the recent study, we observed the downregulation of nucleosome assembly protein 1-like 1 (Nap1l1) in the process of P19CL6 cells' differentiation into cardiomyocytes by proteomics analysis [6]. Nap1, which belongs to nucleosome assembly protein (Nap) family, participates in DNA replication and nucleosome assembly [7]. It has been reported to regulate cell proliferation by interacting with cyclin B and promoting proper assembly of the mitotic spindle [8]. Nap1l1 is highly homologous to Nap1, but the exact mechanism by which Nap1l1 functions is currently unclear. Steer et al. reported that Xenopus NAP1L mRNA is predominantly expressed in oocytes in adults, and it becomes progressively tissue-restricted as embryonic

[a]Shanghai Institute of Cardiovascular Diseases, Zhongshan Hospital and Institutes of Biomedical Sciences, Fudan University, Shanghai, People's Republic of China; [b]Department of Cardiology, Second Affiliated Hospital, Zhejiang University, Hangzhou, People's Republic of China; [c]Department of Physiology and Pathophysiology, Shanghai Medical College, Fudan University, Shanghai, People's Republic of China; [d]Key Laboratory of Stem Cell Biology and Laboratory of Molecular Cardiology, Institute of Health Sciences, Shanghai Institutes for Biological Sciences, Chinese Academy of Sciences and Shanghai Jiao Tong University School of Medicine, Shanghai, People's Republic of China; [e]Department of Cardiovascular Medicine, The University of Tokyo Graduate School of Medicine, Tokyo, Japan

Correspondence: Yunzeng Zou, Ph.D., M.D. or Junbo Ge, Shanghai Institute of Cardiovascular Diseases, Zhongshan Hospital and Institutes of Biomedical Sciences, Fudan University, 180 Feng Lin Road, Shanghai 200032, People's Republic of China. Telephone: 86-21-54237969; Fax: 86-21-54237969; e-mail: zou.yunzeng@zs-hospital.sh.cn

Received April 8, 2013; accepted for publication February 21, 2014; first published online in STEM CELLS *EXPRESS* March 19, 2014.

1066-5099/2014/$30.00/0

http://dx.doi.org/10.1002/stem.1702

development progresses, suggesting that Nap1l1 is a maternal mRNA and has a prominent role in early development [9]. However, there are still few reports about the role of Nap1l1 in heart development or cardiomyocytes differentiation of stem cells.

Our recent data showed that knockdown of Nap1l1 promoted DMSO-induced cardiac-specific proteins expression in P19CL6 cells [6]. To address whether Nap1l1 knockdown could enhance the generation of functional cardiomyocytes from iPSC, we constructed Nap1l1-knockdown iPSC and Nap1l1-overexpressed iPSC, respectively, and observed their differentiation potentials to cardiomyocytes in vitro. The novel role of Nap1l1 in cardiomyocytes differentiation would provide a clue to explore cardiac regeneration strategies.

Materials and Methods

iPSC Culture and Differentiation

The murine iPSC clone iPS-MEF-Ng-20D-17 (APS0001, RIKEN BioResource Center, Ibaraki Japan) was cultured to differentiate into cardiomyocytes by embryonic body (EB) formation. The detailed methods were described in Supporting Information.

Generation of Nap1l1-Knockdown-iPSC, Nap1l1-Overexpression-iPSC, and Inducible Nap1l1-Overexpression-iPSC

Mouse iPSCs were infected with Nap1l1-shRNA or Nap1l1 lentivirus with the selection of puromycin (2 μg/ml, Sigma-Aldrich, St. Louis, MO, USA) or 2 μg/ml puromycin and 200 μg/ml zeocin, and Nap1l1 expression was examined by Western blot analysis. The lentiviral constructs, packaging, and transduction were described in Supporting Information. Quantitative real-time polymerase chain reaction (qRT-PCR), Western blot analysis, flow cytometric analysis, and the cell sorting procedures were available in Supporting Information.

Statistical Analysis

All data were reported as mean ± SEM. The Student's t test was used to determine the significance of differences in comparisons. Values of $p < .05$ were considered to be statistically significant.

Results

Nap1l1 Is Downregulated During the Differentiation Process of iPSC

Our recent study revealed Nap1l1 was downregulated in the process of P19CL6 cells differentiation into cardiomyocytes by proteomics analysis, and knockdown of Nap1l1 promoted cardiac troponin T (cTNT) protein expression in P19CL6 cell treated with DMSO [6]. To learn the expression pattern of Nap1l1 during the differentiation of murine iPSC, we detected the levels of Nap1l1 mRNA in spontaneously formed EBs. As shown in Figure 1A, Nap1l1 mRNA level was sharply decreased in the differentiation process of iPSC from day 4 to day 12 although it was increased quickly from day 0 to day 4 (Fig. 1A). Immunofluorescence analysis showed that the endogenous Nap1l1 was localized mainly in the cytoplasm, despite its sparse distribution in the nucleus of iPSC (Supporting Information Fig. S1A), which is consistent with the subcellular localization of Nap1l1 in HEK293 cells [10]. The distinct dynamic expression of Nap1l1 indicates an important role of the protein in iPSC differentiation.

Additionally, among different organs/tissues of adult mice, Nap1l1 mRNA was expressed abundantly in ovary and at a moderate level in lung but very low in kidney, heart, brain, and blood (Supporting Information Fig. S1B). Further Western blot and qRT-PCR analysis revealed a high expression of Nap1l1 in ESC, iPSC, mesenchymal stem cells, and P19CL6 cells but a low expression in heart tissue at embryonic day 13.5 (E13.5) and 17.5 (E17.5), and very low in heart tissue of postnatal day 1 or adult mice (Fig. 1B). The results indicated that Nap1l1 was expressed highly in pluripotent stem cells or in the organs containing pluripotent cells, and was downregulated during cardiac development, suggesting the downregulation of Nap1l1 is one of the crucial factors for the differentiation of iPSC into cardiomyocytes.

Knockdown or Overexpression of Nap1l1 Does Not Affect the Pluripotent Properties of iPSC

Nap1l1-knockdown-iPSC and Nap1l1-overexpression-iPSC were generated by transfection of Nap1l1-shRNA and Nap1l1-lentiviral vectors into iPSC, respectively. The control iPSCs were infected with shRNA-scramble-pLKO.1 or pLOC lentiviral vectors, respectively. The detailed methods were described in Supporting Information. Western blot analysis showed that the level of Nap1l1 protein was dramatically decreased in shRNA1-Nap1l1-iPSC (Nap1l1-knockdown-iPSC refer to shRNA1-Nap1l1-iPSC in the article) and shRNA2-Nap1l1-iPSC (Supporting Information Fig. S1C, S1D). During the differentiation of iPSC, Nap1l1 expression was obviously downregulated in Nap1l1-knockdown-iPSC while it was significantly increased in Nap1l1-overexpression-iPSC compared with their respective control-iPSC (Supporting Information Fig. S1E).

We next examined whether Nap1l1-knockdown or -overexpression would affect the pluripotency of iPSC. LIF (Leukaemia Inhibitor Factor) cytokine and MEF (Mouse Embryo Fibroblast) in the culture system could sustain the pluripotency of iPSC characterized by the expression of pluripotent markers, such as alkaline phosphatase (AP), Oct4, Nanog, SSEA1, and Sox2. In the presence of LIF and MEF, all the Nap1l1-knockdown-iPSC and Nap1l1-overexpression-iPSC showed the same high mRNA levels of Oct4, Nanog, and Sox2 as in control iPSC (Supporting Information Fig. S1F). We then performed flow cytometry to examine the expression of green fluorescent protein (GFP), a reporter of Nanog-expressed-cells. Both Nap1l1-knockdown-iPSC and Nap1l1-overexpression-iPSC revealed similar profile of GFP expression to that of their control-iPSC, with the frequency of GFP-positive cells at approximately 82% (Fig. 1C). Moreover, immunofluorescence and immunocytochemistry analysis showed neither Nap1l1-knockdown nor Nap1l1-overexpression affected Oct4, SSEA1, and AP expression in iPSC (Fig. 1D). These data suggest that Nap1l1 has little effect on the pluripotent properties of iPSC.

Nap1l1-Knockdown Promotes the Differentiation of iPSC into Functional Cardiomyocytes

We next examined the effect of Nap1l1 on cardiomyocyte differentiation of iPSC after knockdown or overexpression of Nap1l1. To evaluate the differentiation efficiency, iPSCs were

cultured on 96-well plates, and the incidence of the EBs that exhibited spontaneous contraction was counted every day (Fig. 2A). About 200 EBs in each group were counted. Nap1l1-shRNA-EBs began to contract on day 6 and the incidence of contracting EBs increased gradually up to 95% on day 13, while control EBs began to contract on day 7 and reached the maximum of 80% on day 15 (Fig. 2B). However, Nap1l1-overexpression significantly inhibited the incidence of contracting EBs with the maximum of approximately 40% on day 15. Immunofluorescence staining analysis showed that positive area of α-MHC (a marker of mature cardiomyocytes) from shRNA-control-iPSC was two-fold larger than that from Nap1l1-shRNA-iPSC on day 15, but the positive area was significantly smaller in Nap1l1-overexpression EBs than that in control EBs (Fig. 2C). Further fluorescence-activated cell sorting (FACS) analysis showed that the percent of cTNT (the marker of cardiomyocyte) positive cells decreased in Nap1l1-overexpression-EBs but dramatically increased in Nap1l1-knockdown-EBs compared to that in control EBs (Fig. 2D), and re-expression of Nap1l1 in Nap1l1-knockdown-iPSC attenuated the effect of Nap1l1-knockdown on the differentiation of iPSC (Supporting Information Fig. S2A–S2C).

We then detected the expression of cardiac marker mRNA, such as cTNT, α-MHC, β-MHC, atrial natriuretic peptide (ANP), Nkx2.5, GATA4, Tbx5, and Mef2c by qRT-PCR analysis. The results showed that Nap1l1-knockdown in iPSC promoted expressions of these genes while Nap1l1-overexpression strongly inhibited the expressions of these cardiac genes during the differentiation of iPSC into cardiomyocytes (Fig. 2E). Knockdown of Nap1l1 in shRNA1-iPSC, shRNA2-iPSC (Supporting Information Fig. S3), shRNA1-ECs, and shRNA2-ECs (Supporting Information Fig. S4) showed consistent promoting effect on cardiomyocytes differentiation. All these data suggest that early cardiomyocyte differentiation is promoted by Nap1l1 knockdown.

Immunostaining analysis revealed that α-MHC, cTNT, and cardiac troponin complex were expressed in the cytoplasm of cardiomyocytes derived from the control iPSC or Nap1l1-knockdown-iPSC. In addition, positive Cx43 staining was observed on the membrane of myocytes derived from Nap1l1-knockdown- or control-iPSC, which indicated the presence of gap junctions (Supporting Information Fig. S5A). The subcellular localization of cardiac-specific proteins had no difference between control- and Nap1l1-knockdown-iPSC-derived cardiomyocytes.

We next compared the functional properties of cardiomyocytes derived from Nap1l1-knockdown-iPSC and control-iPSC. The beating rate of contracting cardiomyocytes responding to neurohormonal triggers was measured and analyzed by VSL system (900B VSL, ASI, U.S.). Norepinephrine administration (1 μM, $n = 7$) resulted in a significant increase in the beating rate by 102% ± 4% (control group) and 98% ± 5% (Nap1l1-knockdown-iPSC -derived-cardiomyocytes group), respectively (Supporting Information Fig. S5B). In contrast, acetylcholine administration (10 μM, $n = 7$) resulted in a significant decrease in the beating rate by 34% ± 5% and 37% ± 5% from baseline values in control group and Nap1l1-knockdown group, respectively (Supporting Information Fig. S5C). Conduction properties were examined by administration of uncoupler heptanol to control- and Nap1l1-knockdown-iPSC-derived cardiomyocytes (1 mM, $n = 4$). Application of 1 mM heptanol resulted in complete cessation of conduction in both systems ($n = 7$), which was reversible after washout (Supporting Information Fig. S5D). No significant differences were found in their response to the neurohormonal triggers and in their conduction property between the control group and the Nap1l1-knockdown-iPSC-derived-cardiomyocytes group. These results collectively indicate that the Nap1l1-knockdown-iPSC-derived cardiomyocytes display typical cross-striated muscular structure and functional electrophysiological properties.

Nap1l1-Knockdown Promotes Mesodermal Induction of iPSC

To gain further insights into how knockdown of Nap1l1 promotes cardiomyogenesis, the expression of mesoderm specified markers was evaluated. Nap1l1 knockdown in iPSC accelerated and enhanced the expression of Flk-1, Brachyury, Mesp1, and Isl from day 2 to day 4, and it did not affect the rapid downregulation of Brachyury and Mesp1 later. However, Nap1l1 overexpression in iPSC greatly inhibited the upregulation of Flk-1, Brachyury, Mesp1 especially on day 4 (Fig. 3A). FACS analysis revealed that the percentage of Flk1-positive cells was downregulated in Nap1l1-overexpression-EBs and upregulated in Nap1l1-knockdown-EBs compared to that in control-EBs (Fig. 3B), and re-expressing Nap1l1 in Nap1l1-knockdown-iPSC rescued the effect of Nap1/1 (Supporting Information Fig. S2D). We also observed that Nap1l1-knockdown enhanced the induction of endothelial gene (CD31) and smooth muscle genes (Sma and Myh11) expression, while Nap1l1-overexpression had opposite effect (Supporting Information Fig. S6). These results collectively suggest that knockdown of Nap1l1 not only accelerates cardiomyogenesis of iPSC but also promotes iPSC differentiating into mesoderm-derived vascular tissue.

Next, the effects of Nap1l1 on endodermal and ectodermal differentiation were evaluated. FACS analysis revealed that the percentage of CXCR4/C-Kit (endodermal marker) positive cells was little affected either in Nap1l1-knockdown-EBs or in Nap1l1-overexpression-EBs on day 5 (Fig. 3C). The percentage of SOX1 (ectodermal marker) positive cells was hardly detected, which was also less affected by Nap1l1-knockdown or -overexpression (data not shown). These data demonstrate a contributing role of Nap1l1 downregulation in the commitment to mesodermal lineages during primary germ layer induction in vitro.

Nap1l1-Knockdown Promotes Cardiogenesis by Favoring Commitment to Mesodermal Cell Fate

In order to explore whether knockdown of Nap1l1 promotes cardiogenesis by enhancing mesoderm induction process of iPSC, we generated inducible Nap1l1-overexpression-iPSC, in which overexpression of Nap1l1 was induced by incubation with DOX (Supporting Information Fig. S7A, S7B). Inducible overexpression of Nap1l1 by DOX at days 0–5 greatly inhibited the mRNA expressions of mesoderm markers, such as Flk-1, Brachyury, Mesp1, and Isl (Fig. 4A), and cardiac-specific genes, such as MEF2C, NKX2.5, GATA4, TBX5 (Fig. 4B), α-MHC, cTNT, ANP, and β-MHC (Fig. 4C). Further analysis revealed that the inducible Nap1l1-overexpression at days 0–5 significantly inhibited the beating frequency of EBs at day 15 (Fig. 4D), and suppressed the percentage of cTNT-positive cells in EBs (Fig. 4E). However, the inducible Nap1l1-overexpression at days 6–10 has little effects on all these events.

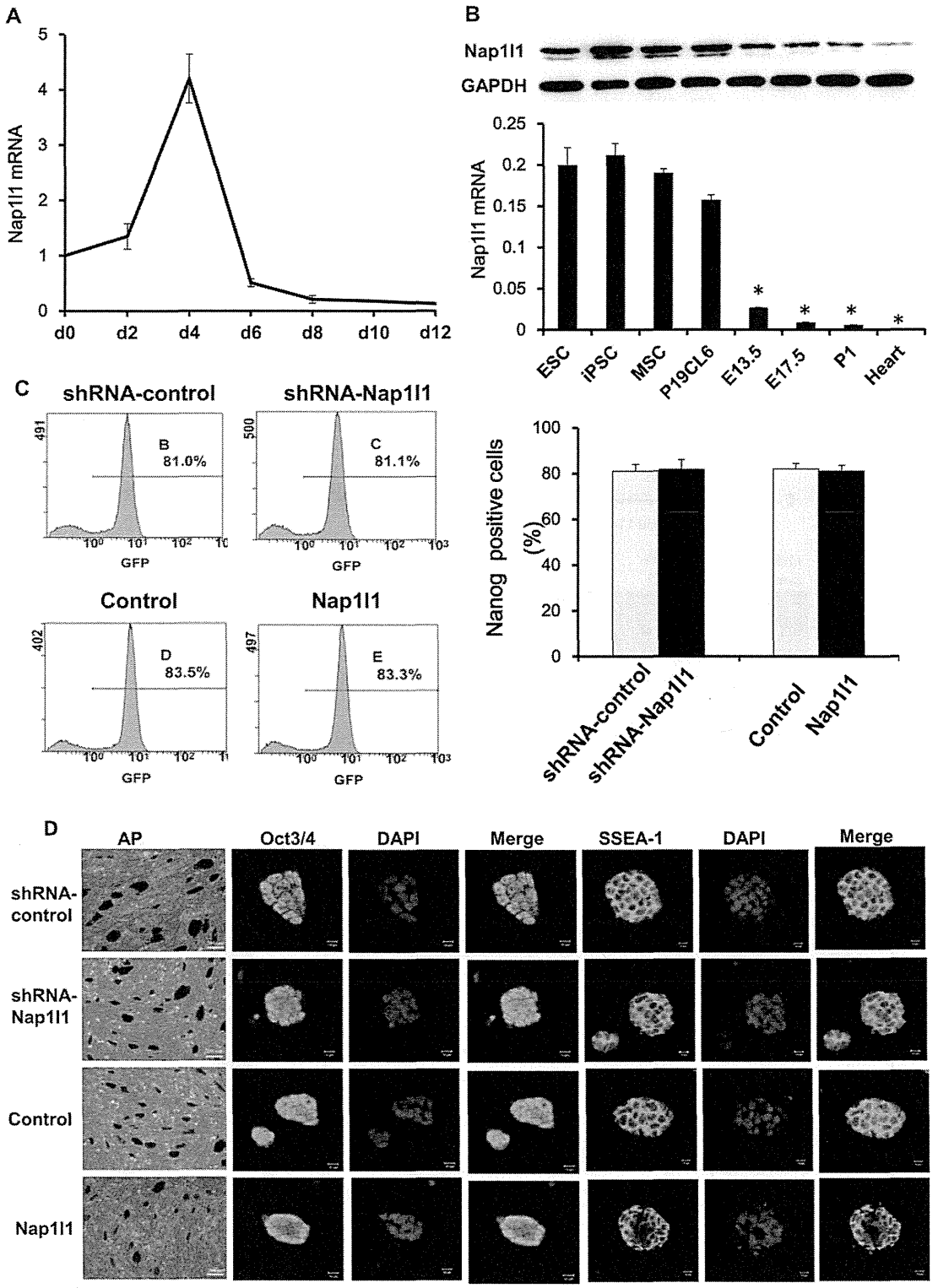

Figure 1. Abundant expression of Nap1l1 in iPSC and its role in pluripotency of iPSC. **(A):** The expression profile of endogenous Nap1l1 during differentiation of mouse iPSC. iPSCs were cultured in the form of embryonic bodies and the Nap1l1 mRNA level at different time points was determined by quantitative real-time polymerase chain reaction (qRT-PCR). Results were represented relative to the value obtained in iPSC at day 0. **(B):** Expression of Nap1l1 in multiple stem cells and heart tissue from different stages of mice was measured by qRT-PCR and Western Blot. E13.5: heart tissue from mouse embryo at day 13.5, E17.5: heart tissue from mouse embryo at day 17.5, P1: heart tissue from postnatal mice at day 1, Heart: adult heart tissue. Each column was normalized by GAPDH. Values are means ± SEM; *, $p < .05$ versus ESC. **(C):** The proportion of GFP-positive cells (EGFP transgene targeted to Nanog) was measured by flow cytometry analysis. **(D):** iPSCs were examined for the expression of AP, Oct4, and SSEA-1. In the presence of LIF and MEF, AP expression (dark purple) was detected by immunocytochemistry method, and Oct4 and SSEA-1 expression (green) were detected by immunofluorescence staining. Scale bars = 10 μm. Nuclei were stained with DAPI (blue). Values are means ± SEM; any experiment was repeated independently at least three times. Abbreviations: AP, alkaline phosphatase; ESC, embryonic stem cell; GFP, green fluorescent protein; iPSC, induced pluripotent stem cell; MSC, mesenchymal stem cell.

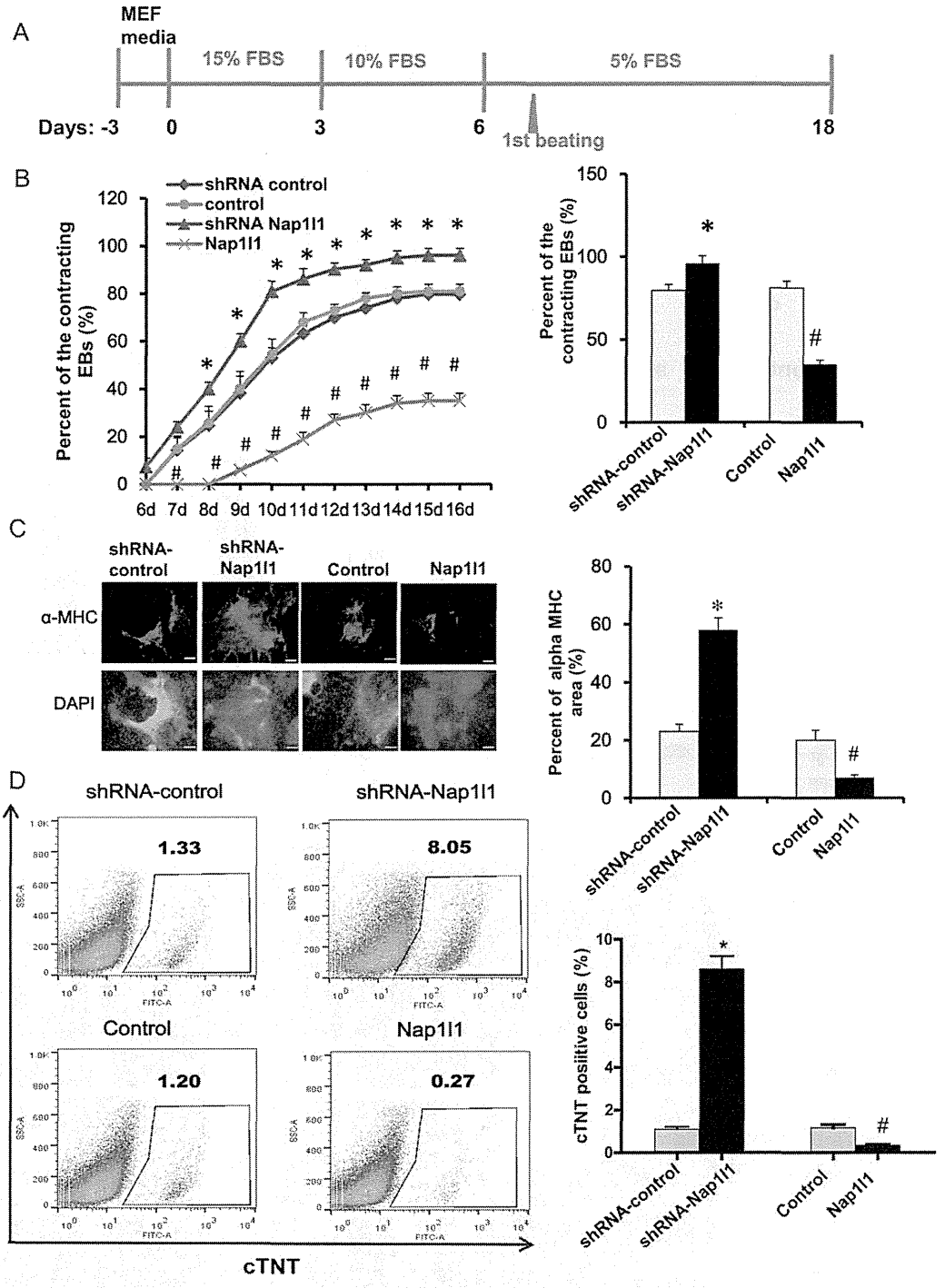

Figure 2. Nap1l1 knockdown promotes the differentiation of mouse induced pluripotent stem cell (iPSC) into cardiomyocytes. **(A):** A schematic presentation of differentiation strategy in vitro for induction of cardiomyocytes from mouse iPSC. **(B):** The incidence of spontaneous contracting EBs (1×10^3 cells/EB) from iPSC was quantified at different time points during differentiation. The graph shows the percentage of contracting EBs at day 15 after EBs formation. **(C):** Immunofluorescent staining of α-MHC in EBs from Nap1l1 knockdown (shRNA-Nap1l1), Nap1l1 overexpression (Nap1l1), and vector controls (shRNA-control and control) iPSC on day 15 of differentiation. Left panels: gross appearance of cardiomyocytes stained with antibody to α-MHC (red), nuclei were stained with DAPI (blue). Scale bars = 200 μm. Right panel: quantitative evaluation of cardiomyocytes induction by analysis of α-MHC positive area. Results were represented relative to the value obtained in shRNA-control iPSC. **(D):** Fluorescence-activated cell sorting analysis of cTNT-positive cells in EBs from Nap1l1 knockdown (shRNA-Nap1l1), Nap1l1 overexpression (Nap1l1), and vector controls (shRNA-control and control) iPSC on day 10 of differentiation. Left panels: the representative pictures. Right panel: the quantitative analysis of the percent of cTNT-positive cells in EBs. **(E):** The mRNA levels of the early and terminal cardiac markers (Nkx2.5, Gata4, Mef2c, Tbx5, α-MHC, β-MHC, cTNT, and ANP) were measured at different time points in differentiation process by quantitative real-time polymerase chain reaction. Each column was normalized by GAPDH. Values are means ± SEM; *, $p < .05$ (shRNA-Nap1l1 vs. shRNA-control); #, $p < .05$ (Nap1l1 vs. control). Any experiment was repeated independently at least three times. Abbreviations: ANP, atrial natriuretic peptide; cTNT, cardiac troponin T; EB, embryonic body.

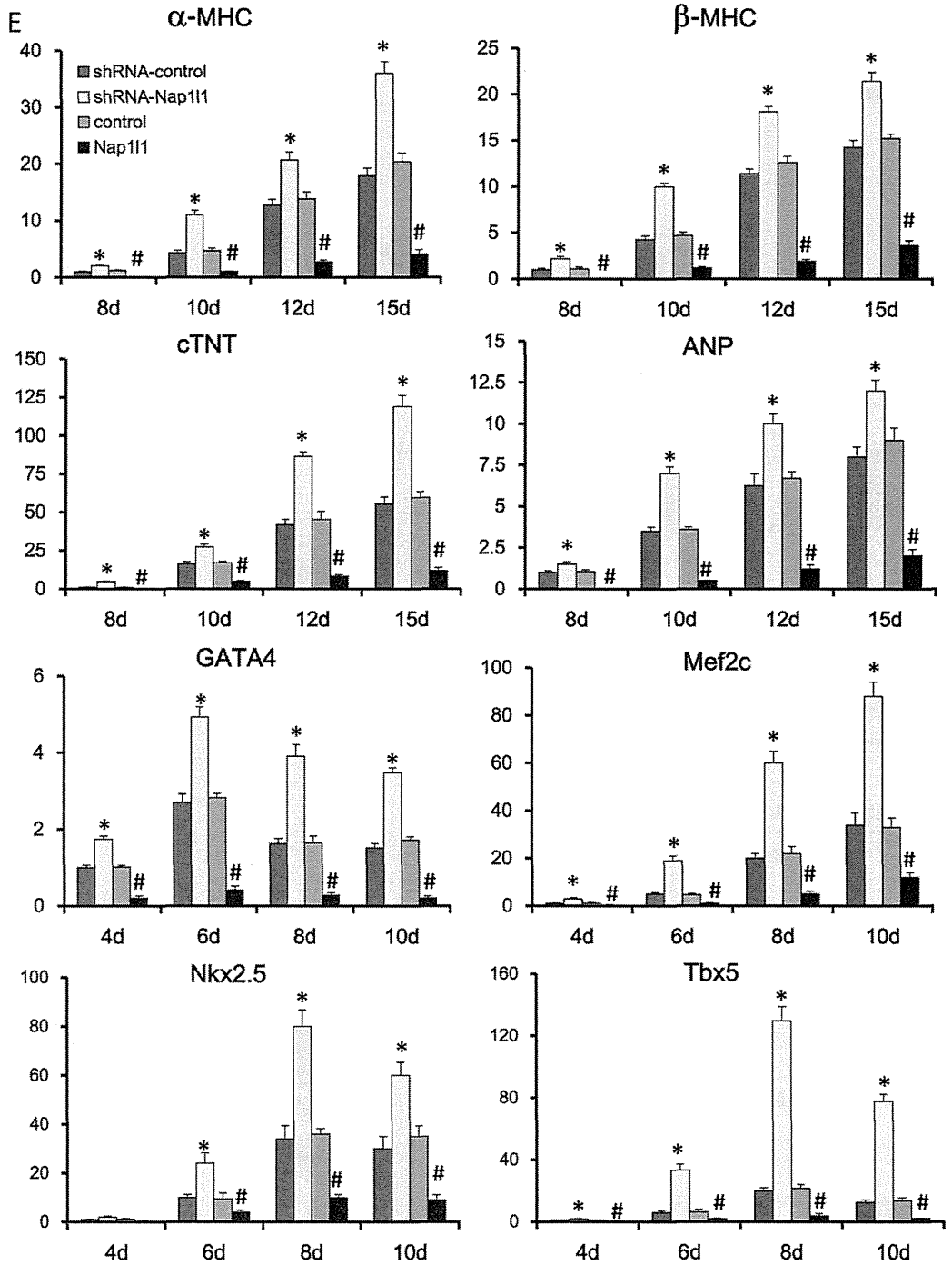

Continued.

We next induced mesoderm differentiation by culturing mouse iPSC with differentiation medium (see Materials and Methods) for 3.5 days. Flk-1-positive mesoderm cells were then selected by FACS and underwent a cardiomyocyte induction protocol involving coculture on OP9 stroma cells. Spontaneously beating cardiomyocytes began to appear after 3–4 days culture. Immunostaining results revealed that α-MHC-positive area showed no difference among the cells from Nap1l1-knockdown-EBs, Nap1l1-overexpression-EBs, and their control-EBs at day 6 (Supporting Information Fig. S8A). The mRNA expression levels of α-MHC, cTNT, ANP, and β-MHC were similar among the cells derived from Nap1l1-knockdown-EBs, Nap1l1-overexpression-EBs, and their control-iPSC at 5 day (Supporting Information Fig. S8B).

Taken together, these data revealed that Nap1l1-downregulation or -overexpression in iPSC did not affect the

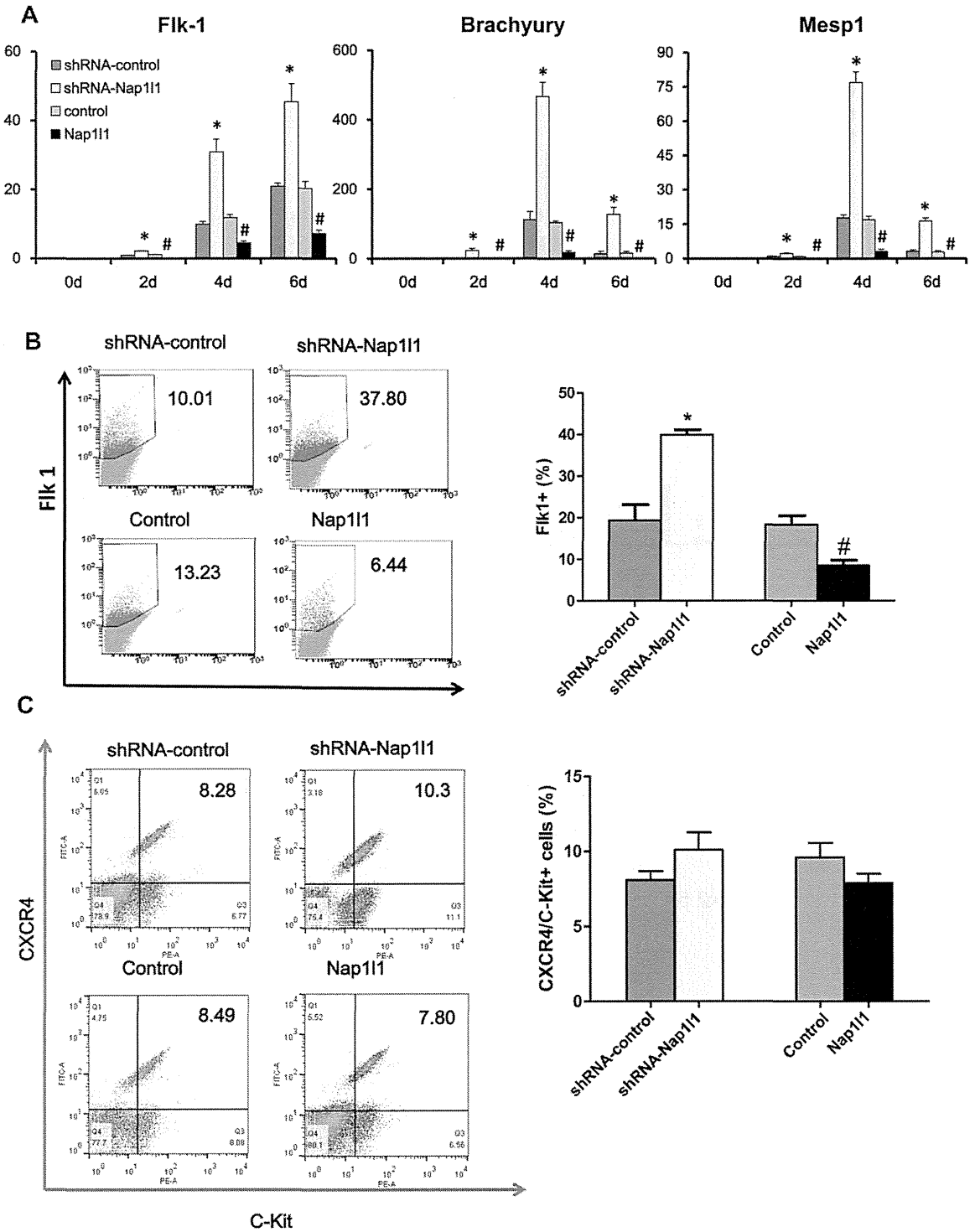

Figure 3. The role of Nap1l1 in the mesodermal and endodermal induction of induced pluripotent stem cell (iPSC). **(A):** Quantitative real-time polymerase chain reaction was performed to detect marker genes of mesoderm, Flk-1, Brachyury, and Mesp1. Each column was normalized by GAPDH. **(B):** Percentage of Flk-1 positive cells in total cells on differentiation day 3.5 by fluorescence-activated cell sorting (FACS) analysis. Left panel: representative images of percent of Flk-1-positive cells. Right panel: quantitative evaluation of Flk-1-positive cells in embryonic bodies (EBs). **(C):** Percentage of CXCR4/C-Kit-positive cells in total cells on differentiation day 5 by FACS analysis. Left panel: representative images of percent of CXCR4/C-Kit-positive cells. Right panel: quantitative evaluation of CXCR4/C-Kit positive cells in EBs. ShRNA-Nap1l1: Nap1l1-knockdown-iPSC, Nap1l1:Nap1l1-overexpression-iPSC. Values are means ± SEM; *, $p < .05$ (shRNA-Nap1l1 vs. shRNA-control); #, $p < .05$ (Nap1l1 vs. control). Any experiment was repeated independently at least three times.

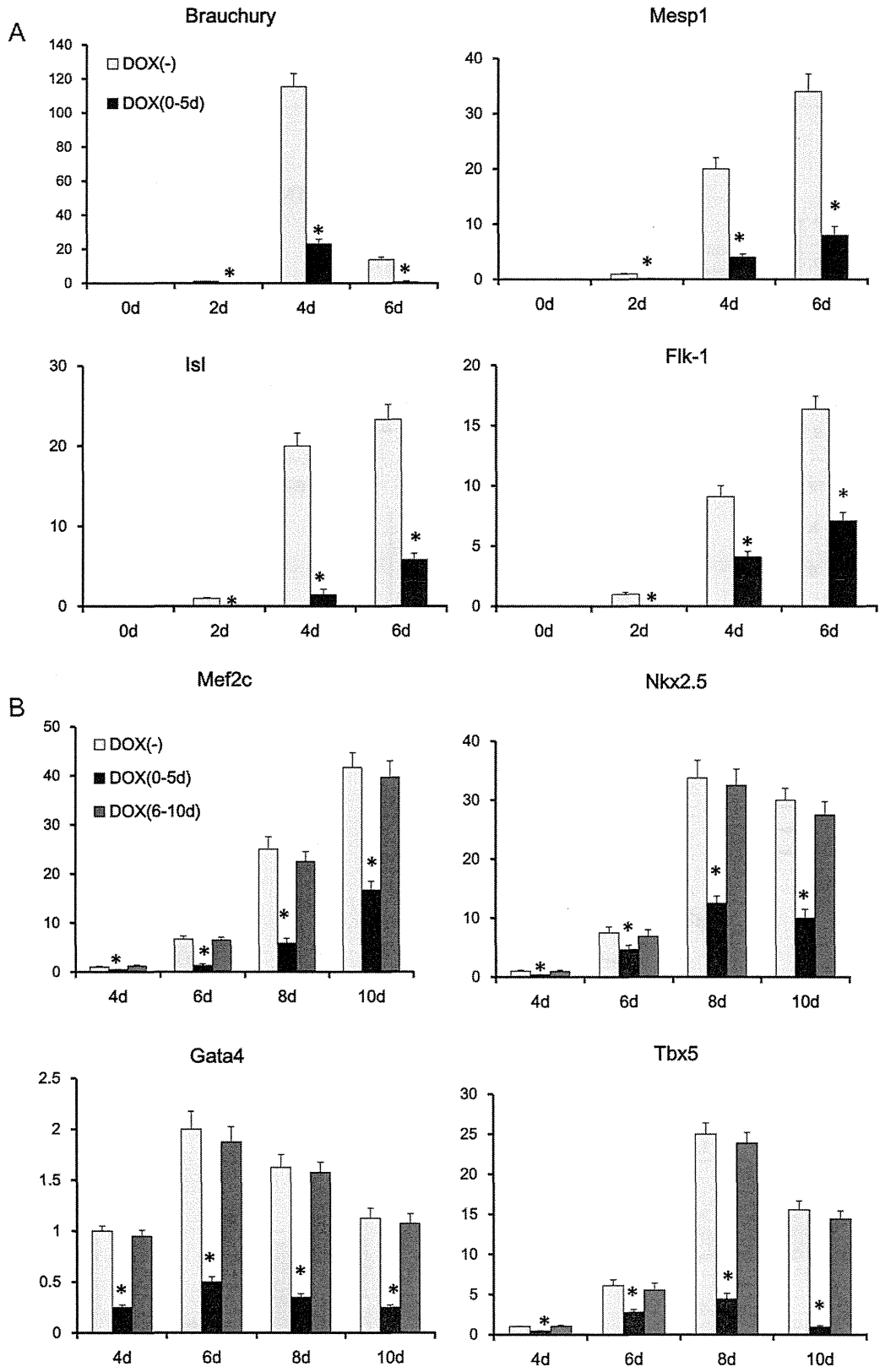

Figure 4. The effect of inducible Nap1l1 overexpression in induced pluripotent stem cell (iPSC) on mesodermal induction and cardiomyocytes differentiation. **(A):** Quantitative real-time polymerase chain reaction (qRT-PCR) was performed to detect marker genes of mesoderm, Brachyury, Mesp1, Isl, and Flk-1, at different time points in differentiation process of iPSC. **(B):** The mRNA levels of cardiac-specific transcription factors (Nkx2.5, Gata4, Mef2c, and Tbx5) were measured at different time points in differentiation process of iPSC by qRT-PCR. Each column was normalized by GAPDH. **(C):** The mRNA levels of cardiac-specific proteins (α-MHC, β-MHC, cTNT, and ANP) were measured at different time points in differentiation process of iPSC by qRT-PCR. **(D):** The incidence of spontaneous contracting EBs from iPSC was quantified at different time points during differentiation. The graph shows the percentage of contracting EBs at day 15 after EBs formation. **(E):** Fluorescence-activated cell sorting analysis of cTNT-positive cells in EBs from iPSC with or without DOX on day 10 of differentiation. Left panels: the representative pictures. Right panel: the quantitative analysis of the percent of cTNT-positive cells in EBs. DOX(−): Inducible-Nap1l1-overexpression-iPSC treated with PBS as control. DOX (0–5): Inducible-Nap1l1-overexpression-iPSCs were treated with DOX from day 0 to day 5. DOX (6–10): Inducible Nap1l1 overexpression iPSCs were treated with DOX from day 6 to day 10. Values are means ± SEM; *, $p < .05$ (vs. DOX(−)). Any experiment was repeated independently at least three times. Abbreviations: ANP, atrial natriuretic peptide; cTNT, cardiac troponin T; EB, embryonic body.

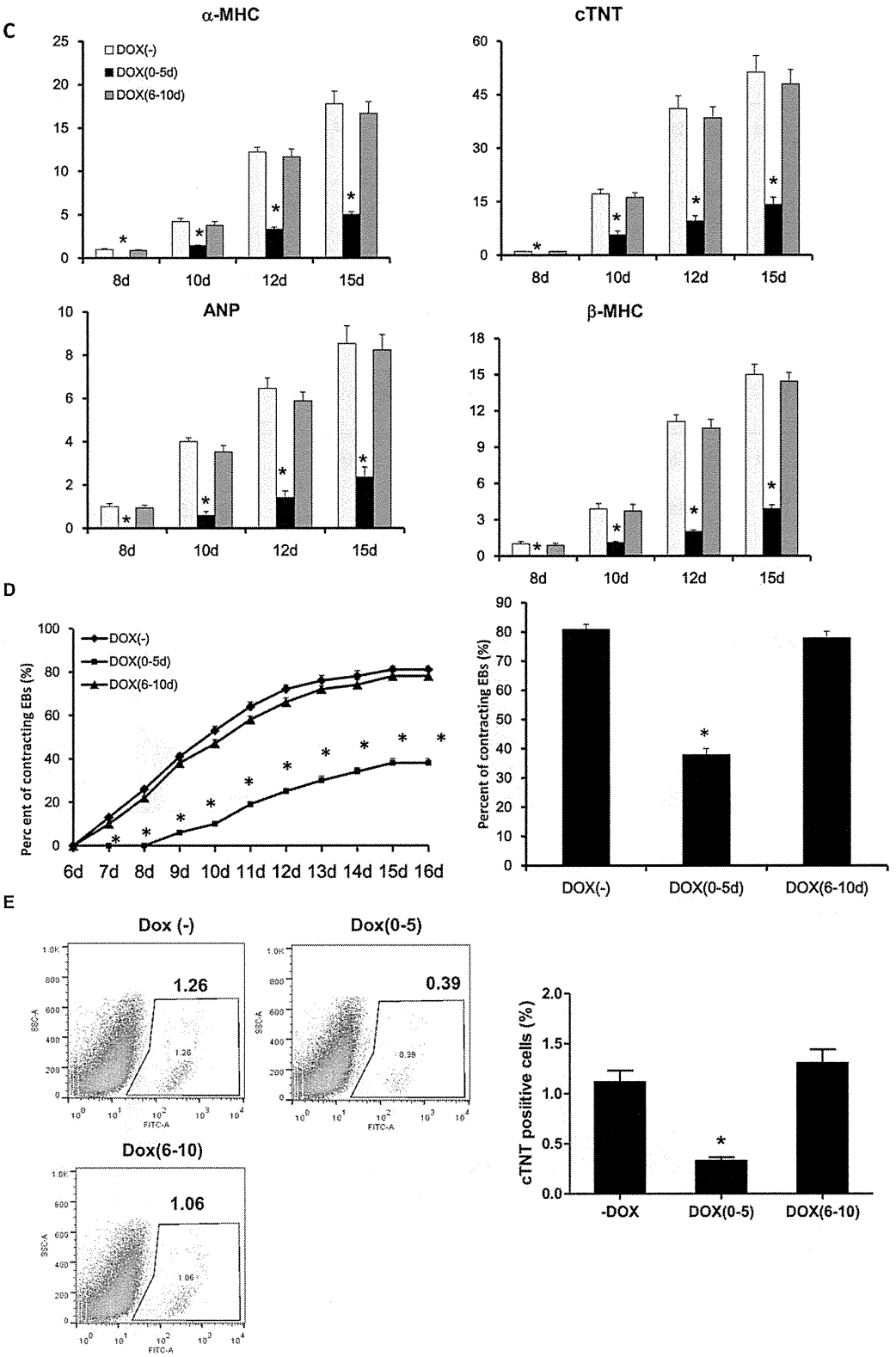

Continued.

differentiation process from mesoderm to cardiomyocytes while Nap1l1-overexpression at early stage inhibited the mesodermal induction and cardiomyocytes differentiation, suggesting that Nap1l1-knockdown promotes cardiomyogenesis by enhancing mesoderm induction process of iPSC.

Active Notch1 Expression Is Regulated by Nap1l1 During the Differentiation of iPSC

Loss of Notch signaling in ESC was recently shown to favor commitment to mesoderm and to induce cardiogenesis [11, 12]. We analyzed the activation of Notch1 during the differentiation of iPSC. Western blot results showed that the expression of active Notch1, Notch intracellular domain (NICD), was increased from day 2 to day 6, and then rapidly downregulated from day 8, which was similar to that of Nap1l1 (Fig. 5A). Nap1l1-knockdown in iPSC significantly inhibited the expression of NICD while Nap1l1-overexpression upregulated the NICD expression (Fig. 5B). We then detected the expression of downstream genes of Notch1. Real-time PCR analysis revealed that Hes1, Hes5, Hey1, and Hey 2 expressions were decreased by Nap1l1-knockdown but they were increased by Nap1l1-overexpression in iPSC (Fig. 5C). To explore whether Notch1 expression was regulated by Nap1l1 during the differentiation of iPSC, we detected NICD expression in Nap1l1-overexpression- or Nap1l1-knockdown-iPSC. From day 2 to day 6 during differentiation of iPSC, Nap1l1-knockdown greatly inhibited the expression while Nap1l1-overexpression increased the expression of NICD (Fig. 5D). Inducible Nap1l1-overexpression by DOX promoted NICD production from day 2 to day 6 during the differentiation of iPSC (Supporting Information Fig. S7C). It suggests that NICD is regulated by Nap1l1 during the differentiation of iPSC.

NICD is yielded by the proteolytic cleavages of Notch with γ-secretase enzyme complex [13]. To explore the effect of Nap1l1 on γ-secretase activity, we used sensitive Notch ΔE-GVP reporter gene assay to monitor γ-secretase-mediated cleavage (site 3 cleavage) of Notch. The cleavage of Notch ΔE-GVP by γ-secretase would release the transcription factor that activates luciferase expression, thereby providing a quantitative measurement of Notch ΔE γ-cleavage. Nap1l1-knockdown or -overexpression of HEK293T cells was transiently transfected with the constructs carrying CMV-β-gal, MH100, and Notch ΔE-GVP. After 48 hours, luciferase activity and β-galactosidase activity were measured. The results showed that luciferase activity was greatly enhanced by Nap1l1-overexpression but it was significantly inhibited by Nap1l1-knockdown (Fig. 5E). It suggests that Nap1l1 induces NICD production by promoting γ-secretase activity.

Notch Inhibitor Reverses Nap1l1-Overexpression-Induced Inhibitory Effects on Mesoderm Induction and Cardiogenesis of iPSC

To confirm the role of Notch signaling in the effect of Nap1l1 on the differentiation of iPSC, the Notch inhibitor was used from day 0 to day 6 during the differentiation of Nap1l1-overexpression-iPSC. DAPT (N-[N-(3,5-difluorophenacetyl)-L-alanyl]-S-phenylglycinet-butyl ester), a γ-secretase inhibitor, greatly reduced the release of NICD in iPSC during differentiation (Fig. 6A). DAPT partly reversed Nap1l1-overexpression-induced downregulation of mesodermal (Brachyury, Mesp1, Isl, and Flk-1) and early cardiogenic markers (GATA4, Nkx2.5, Tbx5, and Mef2c) in iPSC. DAPT alone induced a significant increase in the expression of these genes in iPSC (Fig. 6B), consisting with previous study [12]. Furthermore, DAPT treatment partly abolished the inhibitory effect of Nap1l1-overexpression on the incidence of contracting EBs (Fig. 7A). Consistently, DAPT treatment partly reversed Nap1l1-overexpression-induced decreases of α-MHC-positive area (Fig. 7B) and expressions of α-MHC, cTNT, ANP, and β-MHC (Fig. 7C). In addition, DAPT treatment significantly increased the α-MHC positive area and cardiac-specific genes' expressions in iPSC at day 15 compared to those treated with DMSO, which is also consistent with the previous study. These data suggest that Nap1l1 negatively regulates mesoderm induction and cardiogenesis of iPSC by Notch signaling pathway.

Discussion

In this study, we observed that Nap1l1 was expressed highly in multiple stem cells including iPSC but at very low level in heart tissue and that knockdown of Nap1l1 promoted mesoderm induction and subsequent cardiomyogenesis of murine iPSC by inhibition of Notch signaling. We demonstrate, for the first time, that Nap1l1 plays an essential role in the differentiation of iPSC at early phase in vitro. Our findings thus reveal a novel role of Nap1l1 in mesoderm induction and subsequent cardiomyocytes differentiation of iPSC, which would provide new insights into cardiac regeneration strategies.

The iPSC offers tremendous promise for repairing damaged heart tissues for their capability to differentiate into cardiovascular cells. However, the low efficiency of cardiomyocytes differentiation hinders the clinical application of iPSC technology for cardiac repair strategy. It is critical to identify the inductive or inhibitory effect of various growth factors or proteins on the differentiation of iPSC into cardiomyocytes. Recently, we observed the downregulation of Nap1l1 in the process of P19CL6 cells differentiation into cardiomyocytes by functional proteomics analysis. Knockdown of Nap1l1 promotes DMSO-induced cardiomyocytes differentiation of P19CL6 [6]. Here, we explored the effect of Nap1l1 on the cardiomyocytes differentiation of iPSC. Endogenous Nap1l1 expression was observed at high level in multiple stem cells including iPSC but at very low level in heart tissue including embryonic heart tissue. During the differentiation process of iPSC, Nap1l1 expression was rapidly upregulated at the early stage and then gradually downregulated in the following processes, suggesting a critical role of Nap1l1 downregulation during cardiomyocytes differentiation of iPSC.

Nap1, which belongs to Nap family and is highly conserved from yeast to human, represents the primary chaperone of H2A and H2B and may play a role in cell proliferation, apoptosis, and transcriptional control. Nap1l1 is highly homologous to Nap1 and can also function as histone chaperon [14, 15]. Several studies have identified Nap1l1 being highly expressed in tumors, suggesting the association with tumorigenesis [16]. However, there are few reports about the role of Nap1l1 in the development or the differentiation of stem cells. This study showed that Nap1l1 was expressed abundantly in ovary but lowly in other tissues including heart. The result is consistent with that of Steer study [17]. Steer et al. reported that Xenopus NAP1L (Nap1l1 is one of the family) mRNA is predominantly expressed in oocytes in adults, and it

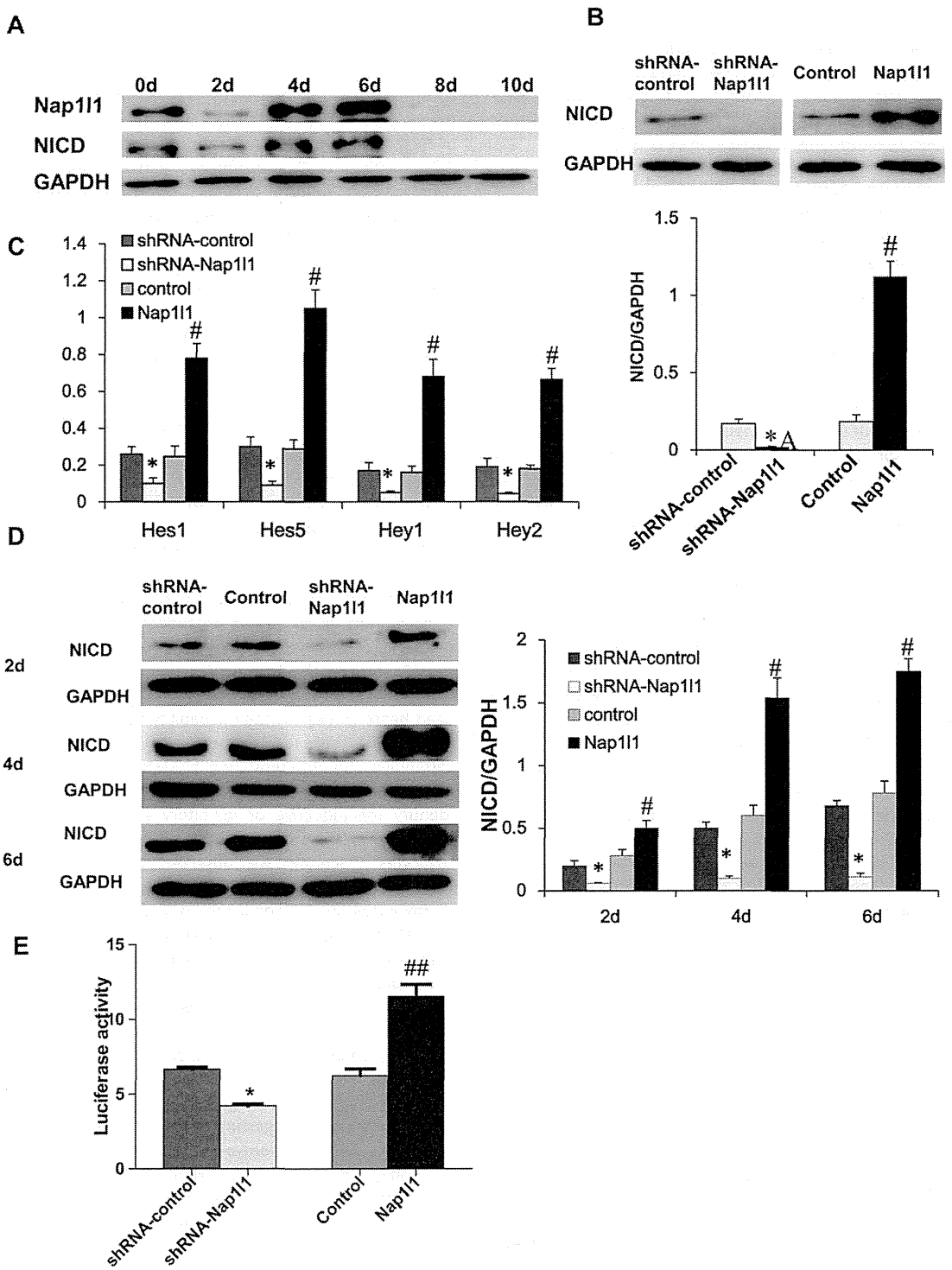

Figure 5. Notch signaling is regulated by Nap1l1 in the differentiation of induced pluripotent stem cell (iPSC). **(A):** The expression of Nap1l1 and activated Notch1, NICD were observed at different time points during differentiation process in iPSC by Western blot analysis. iPSCs were induced to differentiate by embryonic body formation. **(B):** Expression of NICD in Nap1l1-shRNA- and Nap1l1-overexpression-iPSC was analyzed by Western blot. Histogram represented densitometric measurement of specific bands with GAPDH level as control. **(C):** The mRNA levels of known Notch target genes (Hes1, Hes5, Hey1, and Hey2) were measured by quantitative real-time polymerase chain reaction. **(D):** Western blot was used to determine the expression of NICD on days 2, 4, and 6 during iPSC differentiation. Histogram represented densitometric measurement of specific bands with GAPDH level as control. **(E):** γ-Secretase activity was measure by dual luciferase assay. After transfected shRNA-Nap1l1, Nap1l1, or control lentivirus, respectively, for 3 days, HEK293T cells were transfected with CMV-β-gal (Applied Biosystems), MH100, and Notch ΔE-GVP using Fugene transfection reagent. Forty-eight hours later, luciferase activity and β-galactosidase activity of cells extracts were measured. Values are means $\pm$ SEM; *, $p < .05$ (shRNA-Nap1l1 vs. shRNA-control); $^{\#}$, $p < .05$; $^{\#\#}$, $p < .01$ (Nap1l1 vs. control). Any experiment was repeated independently at least three times. Abbreviation: NICD, notch intracellular domain.

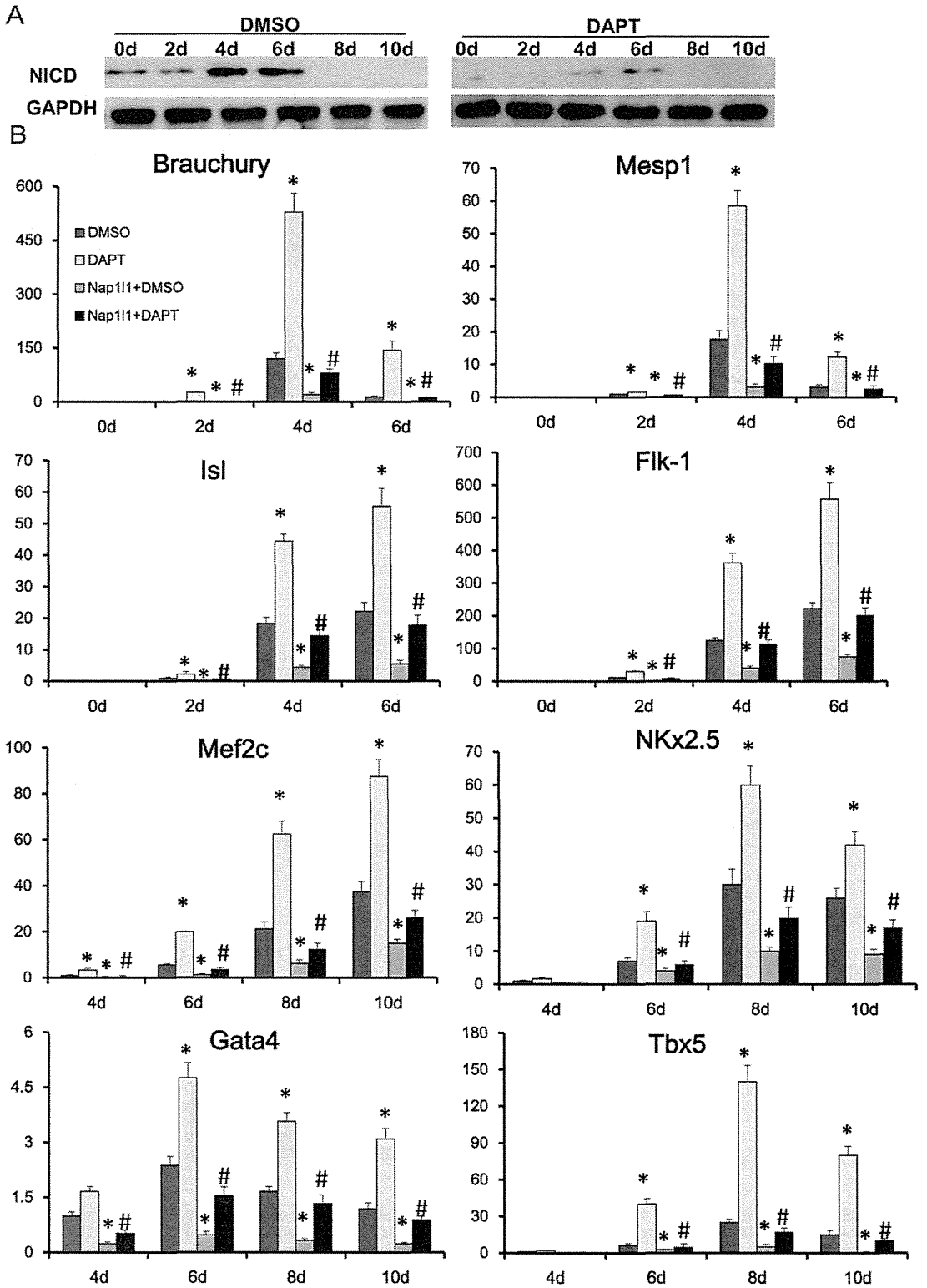

Figure 6. Notch inhibitor partly reversed Nap1l1-overexpression-induced downregulation of cardiac-specific genes in embryonic bodies (EBs). **(A):** Western blot was used to determine the expression of NICD in induced pluripotent stem cell (iPSC) treated with DMSO or DAPT during EBs differentiation. **(B):** The mRNA levels of mesodermal markers (Brachyury, Mesp1, Isl, and Flk-1) and early cardiogenic markers (GATA4, Nkx2.5, Tbx5, and Mef2c) were measured by quantitative real-time polymerase chain reaction during in vitro differentiation of control-iPSC and Nap1l1-overexpression-iPSC treated with DMSO or DAPT. Each column was normalized by GAPDH. Values are means ± SEM; *, $p < .05$ (vs. DMSO); #, $p < .05$ (vs. Nap1l1+DMSO). Any experiment was repeated independently at least three times. Abbreviation: NICD, notch intracellular domain. DAPT: N-[N-(3,5-difluorophenacetyl)-L-alanyl]-S-phenylglycinet-butyl ester.

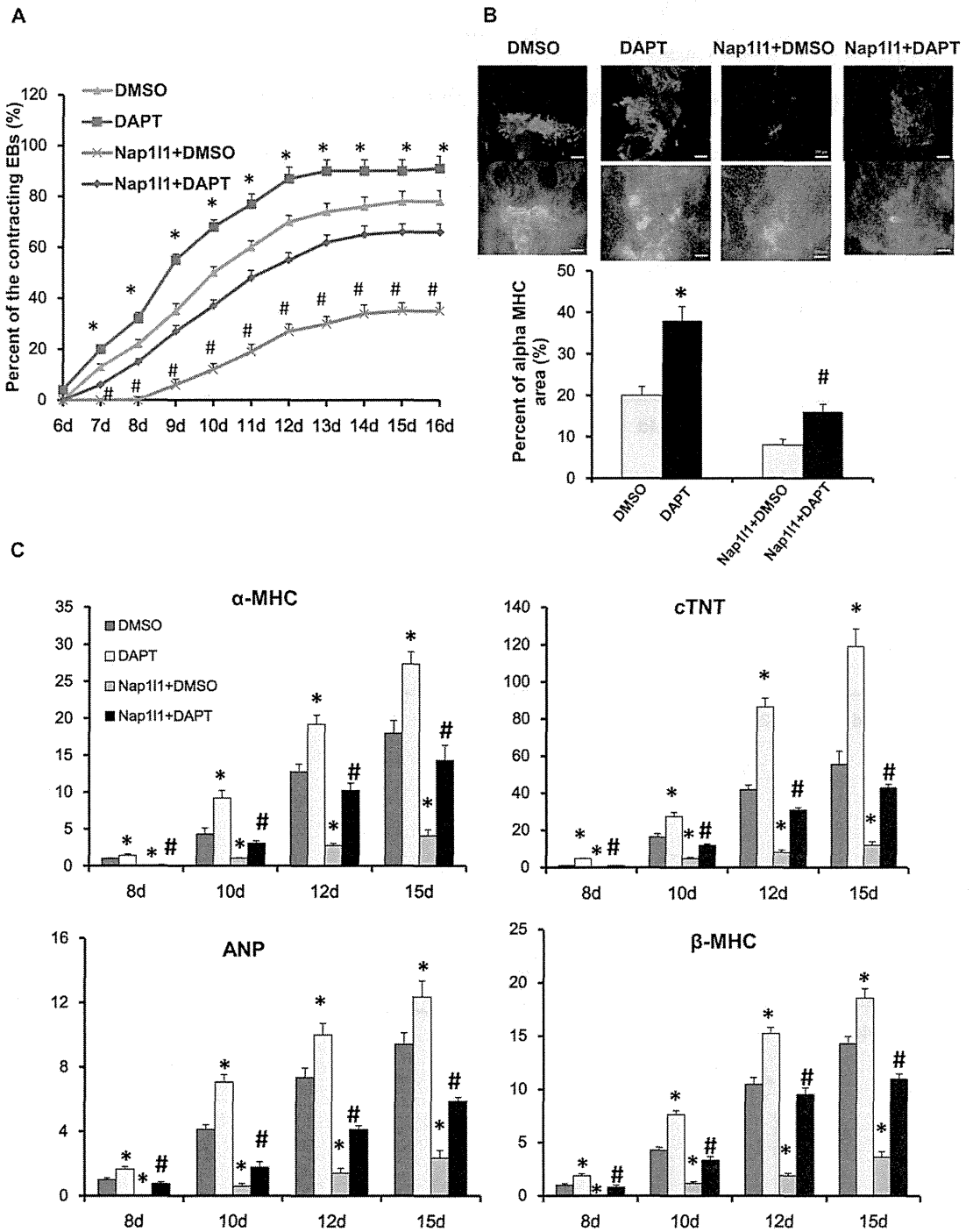

Figure 7. Notch inhibitor partly reversed Nap1l1 overexpression-induced inhibitory effect on cardiomyocytes differentiation of induced pluripotent stem cell (iPSC). **(A):** The incidence of spontaneous contracting EBs (1×10^3 cells/EB) from iPSC and Nap1l1-overexpression-iPSC treated with DMSO or DAPT was quantified at different time points during differentiation. The graph shows the percentage of contracting EBs at day 15 after EBs forming. **(B):** Immunofluorescent staining of α-MHC in EBs from control iPSC and Nap1l1-overexpression-iPSC treated with DMSO or DAPT on day 15 of differentiation. Left panels: gross appearance of cardiomyocytes stained with antibody to α-MHC (red), nuclei were stained with DAPI (blue). Scale bars = 200 μm. Right panel: quantitative evaluation of cardiomyocytes induction by analysis of α-MHC-positive area. **(C):** The mRNA levels of terminal cardiac markers (α-MHC, β-MHC, cTNT, and ANP) were measured from day 8 to day 15 of differentiation by quantitative real-time polymerase chain reaction. Each column was normalized by GAPDH. Values are means ± SEM; *, $p < .05$ (vs. DMSO); #, $p < .05$ (vs. Nap1l1+DMSO). Any experiment was repeated independently at least three times. Abbreviations: ANP, atrial natriuretic peptide; cTNT, cardiac troponin T; EB, embryonic body.

becomes progressively tissue-restricted as embryonic development progresses, suggesting that Nap1l1 is a maternal mRNA and has a prominent role in early development [9]. But the potential mechanisms are unclear.

To better understand the role of Nap1l1 during cardiomyocyte differentiation of iPSC, we generated Nap1l1-knockdown- and Nap1l1-overexpression-iPSC to observe their differentiation potential to cardiomyocytes in vitro. Neither Nap1l1-knockdown nor Nap1l1-overexpression affected the pluripotency of iPSC. However, Nap1l1-knockdown significantly enhanced cardiac differentiation rate of iPSC, characterized by the increased incidence of beating EBs, the increased number of positive cTNT, and larger α-MHC-positive area. Further analysis showed that Nap1l1-knockdown promoted the expression of key cardiac transcription factors, Nkx2.5, GATA4, Tbx5, and Mef2c which are required for cardiac commitment to mesodermal cells. But Nap1l1-overexpression greatly inhibited the cardiogenic differentiation of iPSC. Cardiomyocytes derived from Nap1l1-knockdown-iPSC exhibited typical cross-striated muscle structure and functional electrophysiological properties, indicating that these cardiomyocytes are highly differentiated and functionally responsive cardiomyocytes.

We then detected the effect of Nap1l1 on lineage differentiation of iPSC. The results showed that Nap1l1-knockdown in iPSC had little effect on the endoderm development, but it promoted mesodermal induction by enhancing the number of Flk-1 positive cells and the expression of mesodermal marker genes including Flk-1, Brachyury, and Mesp1. We also observed that Nap1l1-knockdown enhanced the induction of endothelial and smooth muscle genes expression. These data suggest that downregulation of Nap1l1 not only accelerates cardiomyogenesis but also promotes mesoderm-derived vascular differentiation.

To explore whether Nap1l1-knockdown promotes cardiac differentiation secondary to mesodermal induction, we generated inducible Nap1l1-overexpression-iPSC and observed that Nap1l1-overexpression at early stage greatly inhibited mesodermal induction and cardiomyocyte differentiation of iPSC while Nap1l1-overexpression at late stage did not affect the process. To explore whether Nap1l1 regulates cardiomyocytes differentiation from mesodermal cell, we purified Flk-1-positive cells induced from Nap1l1-knockdown- or overexpression-iPSC and observed the cardiomyocytes differentiation. There was no obvious difference in cardiomyocytes differentiation among mesoderm cells originated from Nap1l1-knockdown-, Nap1l1-overexpression-, and control-iPSC, suggesting that knockdown of Nap1l1 promotes cardiogenesis by favoring commitment to a mesodermal cell fate.

In the mouse embryo, lineage decision requires the cell-cell interaction that is influenced by coordinated cell migration and cellular neighborhood, and mediated by the key WNT, FGF, and TGF-β signaling pathways [27, 28] which are involved in cardiac development. Notch could crosstalk with these pathways including WNT, BMP, and TGF-β to regulate the cell fate [19, 29]. Notch also has been reported to play an important role in the commitment between mesodermal and neuroectodermal lineages and seems to regulate cardiogenesis in mesodermal precursors. Inhibition of Notch signaling promotes mesodermal induction and cardiomyocytes differentiation of ESC [11, 20], which is similar to those induced by Nap1l1-knockdown in iPSC. This study revealed that Nap1l1-knockdown in iPSC greatly inhibited the expression of NICD and its downstream genes while Nap1l1-overexpression showed opposite effects. NICD yielded by the proteolytic cleavages of Notch with γ-secretase enzyme complex, translocates to the nucleus, and activates Hes/Hey transcription [13], which leads to repression of Hes/Hey target genes such as tissue-specific transcriptional activators, thereby preventing differentiation [21]. In addition, Notch has been reported to regulate lineage decision by control of asymmetric division. Cells demonstrating active Notch signaling during asymmetric division are prevented from committing to a particular fate [13]. So we speculate that Nap1l1-knockdown promotes mesodermal induction by inhibition of NICD. γ-Secretase enzyme complex mediates the second cleavage of Notch receptor to release NICD [13]. In this study, luciferase reporter assay revealed that Nap1l1-knockdown inhibited γ-secretase enzyme activity while Nap1l1-overexpression increased the enzyme activity in HEK 293T cells. Further analysis revealed that DAPT, γ-secretase inhibitor, greatly inhibited NICD expression and reversed Nap1l1-overexpression-induced inhibitory effect on mesoderm induction and cardiomyocyte differentiation of iPSC. These data indicate that knockdown of Nap1l1 inhibits the activity of γ-secretase, downregulates the NICD expression, and promotes mesodermal induction and cardiomyocytes differentiation of iPSC.

In this study, we did not further explore how Nap1l1 regulates γ-secretase activity. A functional γ-secretase complex can be reconstituted by four proteins: presenilin (PS1 or PS2), nicastrin, Aph-1, and Pen-2 [22]. PS endoproteolysis is an important step in the formation of an active γ-secretase complex [23], the mechanisms of which remain largely elusive. Nicastrin, an essential component of γ-secretase, has been reported to be required for the cleavage of the intracellular fragment from Notch. It binds to membrane-tethered forms of Notch and modulates the S3-site cleavage of Notch, and thereby produces NICD [23]. Nap1l1 protein has the capacity to augment the activity of different p300 targets, including p53 and E2F [24, 25] in cell cycle regulation, but whether Nap1l1 promotes PS endoproteolysis or the interaction between nicastrin and Notch to facilitate γ-secretase proteolysis remains to be elucidated. In addition, Notch receptor binds to ligands such as Delta (Dl) or Jagged and undergoes successive proteolytic cleavages which lead to the release of NICD. Nap1l1 might also regulate Notch-ligand interaction and induce the production of NICD to regulate the differentiation of iPSC.

Moreover, Nap1l1 has been reported to mediate nucleosome formation or disassembly by associating with various histone [19]. Meshorer et al. reported that prevention of chromatin proteins from assembly into chromatin accelerates differentiation, while restriction of linker histone in ESCs blocks differentiation. These data imply that the dynamic nature of chromatin is functionally important for stem cell differentiation [18]. But the detailed mechanisms are unclear. It is of great significance to further explore the interaction among Nap1l1, chromatin remodeling, and mesodermal cell fate.

Conclusion

This study indicates that knockdown of Nap1l1 dramatically promotes iPSC differentiation into functional cardiomyocytes

by enhancing mesoderm induction, which is regulated by Notch signaling. Thus, it suggests that Nap1l1-downregulation-mediated mesodermal induction and cardiogenic differentiation would be a mandatory step for cardiac regeneration.

Acknowledgments

We thank Ying Chen, Wenwei Wang, and Yonghua Liang for excellent technical assistance. We thank Dr. Gang Pei and Dr. Jiucheng Kang for kindly providing iPS-R-B1 and plasmids (MH100 and Notch ΔE-GVP), and thank Dr. Gustavo Mostoslavsky and Dr. Allan Bradley for kindly providing pHAGE2-Tet-STEMCCA plasmid and vector–pPB-CAG-IRES, respectively. This work was supported by National Basic Research Program of China (2010CB945500), National Natural Science Foundation of China (30930043 and 81220108003), Doctoral Fund of Ministry of Education of China (20110071110051 and 200802461124), and Science and Technology Commission of Shanghai Municipality (08dj1400504, 13JC1401703, and 11JC1402400).

Author Contributions

H.G.: conception and design, collection and/or assembly of data, data analysis and interpretation, manuscript writing, and final approval of manuscript; Y.Y.: collection and/or assembly of data, data analysis and interpretation, and manuscript writing; F.B. and Y.X.: collection and/or assembly of data and data analysis and interpretation; Y.P., L.L., G.Z., X.S., and Z.C.: collection and/or assembly of data; H.M., C.Y., Y.D., and Y.Y.: data analysis and interpretation; Y.Zhu, H.Y., and I.K.: provision of study materials; J.G.: data analysis and interpretation and administrative support. Y.Zou: conception and design, data analysis and interpretation, manuscript writing, and final approval of manuscript. H.G., Y.Y., B.F., and Y.X. contributed equally to this work.

Disclosure of Potential Conflicts of Interest

The authors indicate no potential conflicts of interest.

References

1 Templin C, Luscher TF, Landmesser U. Cell-based cardiovascular repair and regeneration in acute myocardial infarction and chronic ischemic cardiomyopathy-current status and future developments. Int J Dev Biol 2011;55:407–417.
2 Mali P, Ye Z, Hommond HH et al. Improved efficiency and pace of generating induced pluripotent stem cells from human adult and fetal fibroblasts. Stem Cells 2008; 26:1998–2005.
3 Vallier L, Touboul T, Brown S et al. Signaling pathways controlling pluripotency and early cell fate decisions of human induced pluripotent stem cells. Stem Cells 2009;27: 2655–2666.
4 Narazaki G, Uosaki H, Teranishi M et al. Directed and systematic differentiation of cardiovascular cells from mouse induced pluripotent stem cells. Circulation 2008;118: 498–506.
5 Zhang J, Wilson GF, Soerens AG et al. Functional cardiomyocytes derived from human induced pluripotent stem cells. Circ Res 2009;104:e30–41.
6 Li L, Gong H, Yu H et al. Knockdown of nucleosome assembly protein 1-like 1 promotes dimethyl sulfoxide-induced differentiation of P19CL6 cells into cardiomyocytes. J Cell Biochem 2012;113:3788–3796.
7 Park YJ, Luger K. Structure and function of nucleosome assembly proteins. Biochem Cell Biol 2006;84:549–558.
8 Altman R, Kellogg D. Control of mitotic events by Nap1 and the Gin4 kinase. J Cell Biol 1997;138:119–130.
9 Steer WM, Abu-Daya A, Brickwood SJ et al. Xenopus nucleosome assembly protein becomes tissue-restricted during development and can alter the expression of specific genes. Mech Dev 2003;120:1045–1057.
10 Okada M, Hozumi Y, Ichimura T et al. Interaction of nucleosome assembly proteins abolishes nuclear localization of DGKzeta by attenuating its association with importins. Exp Cell Res 2011;317:2853–2863.
11 Nemir M, Croquelois A, Pedrazzini T, et al. Induction of cardiogenesis in embryonic stem cells via downregulation of Notch1 signaling. Circ Res 2006;98:1471–1478.
12 Jang J, Ku SY, Kim JE, et al. Notch inhibition promotes human embryonic stem cell-derived cardiac mesoderm differentiation. Stem Cells 2008;26:2782–2790.
13 Artavanis-Tsakonas S, Rand MD, Lake RJ. Notch signaling: Cell fate control and signal integration in development. Science 1999; 284:770–776.
14 Simon HU, Mills GB, Kozlowski M, et al. Molecular characterization of hNRP, a cDNA encoding a human nucleosome-assembly-protein-I-related gene product involved in the induction of cell proliferation. Biochem J 1994;297:389–397.
15 Okuwaki M, Kato K, Nagata K. Functional characterization of human nucleosome assembly protein 1-like proteins as histone chaperones. Genes Cells 2010;15:13–27.
16 Attia M, Rachez C, Avner P et al. Nucleosome assembly proteins and their interacting proteins in neuronal differentiation. Arch Biochem Biophys 2013;534:20–26.
17 Steer WM, Abu-Daya A, Brickwood SJ, et al. Xenopus nucleosome assembly protein becomes tissue-restricted during development and can alter the expression of specific genes. Mech Dev 2003;120:1045–1057.
18 Meshorer E, Yellajoshula D, George E et al. Hyperdynamic plasticity of chromatin proteins in pluripotent embryonic stem cells. Dev Cell 2006;10:105–116.
19 Pedrazzini T. Control of cardiogenesis by the notch pathway. Trends Cardiovasc Med 2007;17:83–90.
20 Lowell S, Benchoua A, Heavey B, et al. Notch promotes neural lineage entry by pluripotent embryonic stem cells. PLoS Biol 2006;4:e121.
21 Kathiriya IS, King IN, Murakami M, et al. Hairy-related transcription factors inhibit GATA-dependent cardiac gene expression through a signal-responsive mechanism. J Biol Chem 2004;279:54937–54943.
22 Kimberly WT, LaVoie MJ, Ostaszewski BL et al. Gamma-secretase is a membrane protein complex comprised of presenilin, nicastrin, Aph-1, and Pen-2. Proc Natl Acad Sci USA 2003;100:6382–6387.
23 Edbauer D, Winkler E, Haass C et al. Presenilin and nicastrin regulate each other and determine amyloid beta-peptide production via complex formation. Proc Natl Acad Sci USA 2002;99: 8666–8671.
24 Shikama N, Chan HM, Krstic-Demonacos M et al. Functional interaction between nucleosome assembly proteins and p300/CREB-binding protein family coactivators. Mol Cell Biol 2000;20:8933–8943.
25 Liu X, Zhao X, Zeng X et al. Beta-arrestin1 regulates gamma-secretase complex assembly and modulates amyloid-beta pathology. Cell Res 2013;23:351–365.
26 Yuasa S, Itabashi Y, Koshimizu U, et al. Transient inhibition of BMP signaling by Noggin induces cardiomyocyte differentiation of mouse embryonic stem cells. Nat Biotechnol 2005;23:607–611.
27 Tran TH, Wang X, Browne C, et al. Wnt3a-induced mesoderm formation and cardiomyogenesis in human embryonic stem cells. Stem Cells 2009;27:1869–1878.
28 Dell'Era P, Ronca R, Coco L, et al. Fibroblast growth factor receptor-1 is essential for in vitro cardiomyocyte development. Circ Res. 2003;93:414–420.


See www.StemCells.com for supporting information available online.

Comparison of 5-Year Survival After Acute Myocardial Infarction Using Angiotensin-Converting Enzyme Inhibitor Versus Angiotensin II Receptor Blocker

Masahiko Hara, MD[a], Yasuhiko Sakata, MD, PhD[a,b,c,*], Daisaku Nakatani, MD, PhD[a], Shinichiro Suna, MD, PhD[a], Masaya Usami, MD, PhD[a], Sen Matsumoto, MD, PhD[a], Toshifumi Sugitani, MSc[d], Masami Nishino, MD, PhD[e], Hiroshi Sato, MD, PhD[f], Tetsuhisa Kitamura, MD, MSc, DrPH[g], Shinsuke Nanto, MD, PhD[a,b], Toshimitsu Hamasaki, PhD[d], Masatsugu Hori, MD, PhD[h], and Issei Komuro, MD, PhD[i], on behalf of the OACIS Investigators

Few studies have investigated whether angiotensin II receptor blocker (ARB) is a practical alternative to angiotensin-converting enzyme inhibitor (ACEI) for long-term use after acute myocardial infarction (AMI) in real-world practice in the percutaneous coronary intervention era. We compared 5-year survival benefits of ACEI and ARB in patients with AMI registered in the Osaka Acute Coronary Insufficiency Study. Study subjects were divided into 3 groups: ACEI (n = 4,425), ARB (n = 2,158), or patients without either drug (n = 2,442). A total of 661 deaths were recorded. Cox regression analysis revealed that treatment with either ACEI or ARB was associated with reduced 5-year mortality (adjusted hazard ratio [HR] 0.70, 95% confidence interval [CI] 0.58 to 0.83, p <0.001 and HR 0.79, 95% CI 0.64 to 0.98, p = 0.03, respectively). However, Kaplan-Meier estimates and Cox regression analyses based on propensity score revealed that ACEI was associated with better survival than ARB from 2 to 5 years after survival discharge (adjusted HR 0.53, 95% CI 0.38 to 0.74, p <0.001). These findings were confirmed in a propensity score–matched population. In conclusion, treatment with ACEI was associated with better 5-year survival after AMI. **(Am J Cardiol 2014;114:1–8)**

Angiotensin-converting enzyme inhibitor (ACEI) was the first clinically approved renin-angiotensin-aldosterone system (RAS) inhibitor, and much evidence presented in the 1990s and early 2000s have demonstrated the effectiveness of ACEI for improving cardiovascular disease–related morbidity and mortality.[1–5] Angiotensin II receptor blocker (ARB) has also been examined clinically for cardiovascular disease treatment.[6–10] Based on the results of 2 randomized clinical trials (RCTs) such as Optimal Trial in Myocardial Infarction with Angiotensin II Antagonist Losartan (OPTIMAAL) and the Valsartan in Acute Myocardial Infarction (VALIANT), which examined clinical impacts of ARB after acute myocardial infarction (AMI), the international guidelines recommend that ACEI should be used as the first-line treatment after AMI and that ARB should be considered in patients who are intolerant to ACEI therapy.[6,7,11,12] We investigated whether ACEI and ARB had comparable long-term benefits in a large cohort of post-AMI patients registered in the Osaka Acute Coronary Insufficiency Study (OACIS).[13,14]

Methods

The OACIS is a prospective, multicenter, observational study enrolling consecutive patients with AMI at 25 collaborating hospitals in the Osaka region of Japan.[13,14] The OACIS is registered with the University Hospital Medical Information Network Clinical Trials Registry (UMIN-CTR) in Japan (ID: UMIN000004575). Details of OACIS are described elsewhere (Supplementary Material).[13,14]

The diagnosis of AMI was based on the World Health Organization criteria,[15] which required 2 of the following 3 criteria to be met: (1) clinical history of central chest pressure, pain, or tightness lasting ≥30 minutes; (2) ST-segment elevation >0.1 mV in at least 1 standard or 2 precordial leads; and (3) an increase in serum creatine phosphokinase concentration of more than twice the normal laboratory value. Research cardiologists and trained research nurses recorded data concerning sociodemographic variables, medical

Departments of [a]Cardiovascular Medicine, [b]Advanced Cardiovascular Therapeutics, and [d]Biomedical Statistics and [g]Division of Environmental Medicine and Population Sciences, Department of Social and Environmental Medicine, Osaka University Graduate School of Medicine, Suita, Japan; [c]Department of Cardiovascular Medicine, Tohoku University Graduate School of Medicine, Sendai, Japan; [e]Division of Cardiology, Osaka Rosai Hospital, Sakai, Japan; [f]School of Human Welfare Studies, Kwansei Gakuin University, Nishinomiya, Japan; [h]Osaka Prefectural Hospital Organization, Osaka Medical Center for Cancer and Cardiovascular Diseases, Osaka, Japan; and [i]Department of Cardiovascular Medicine, The University of Tokyo Graduate School of Medicine, Tokyo, Japan. Manuscript received February 22, 2014; revised manuscript received and accepted March 25, 2014.

This work was supported by Grants-in-Aid for University and Society Collaboration (#19590816 and #19390215) from the Japanese Ministry of Education, Culture, Sports, Science and Technology, Tokyo, Japan.

See page 7 for disclosure information.

*Corresponding author: Tel: (+81) 22-717-7152; fax: (+81) 22-717-7156.

E-mail address: sakatayk@cardio.med.tohoku.ac.jp (Y. Sakata).

0002-9149/14/$ - see front matter
http://dx.doi.org/10.1016/j.amjcard.2014.03.055

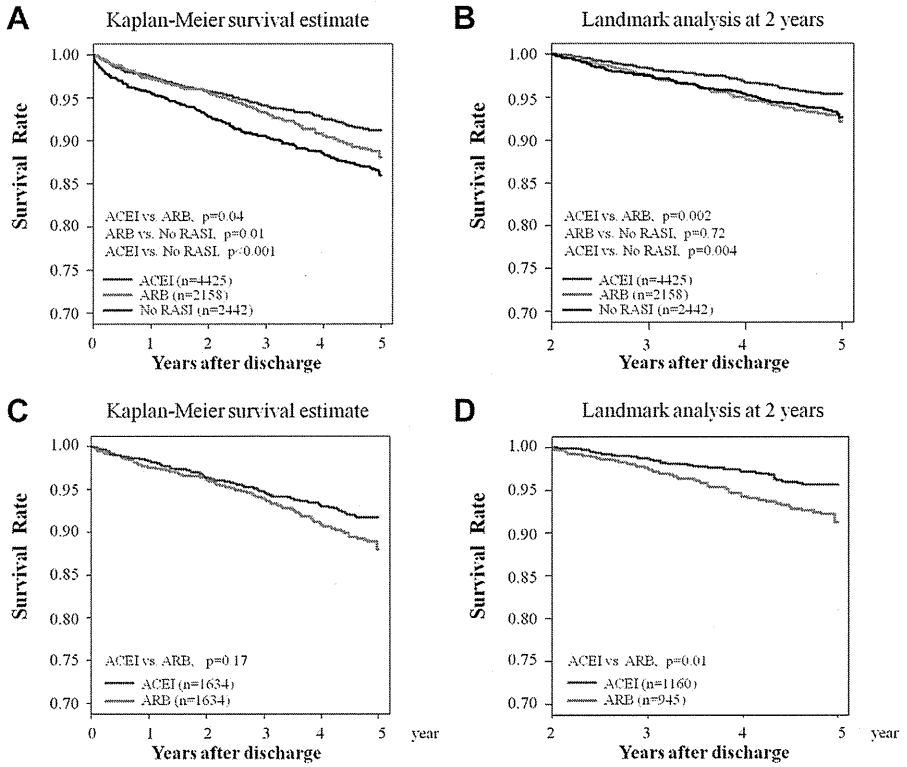

Figure 1. Kaplan-Meier survival estimates and landmark analysis results after survival discharge for AMI in the entire study population *(A* and *B)* and the PS-matched samples *(C* and *D)*. RASI = renin-angiotensin-aldosterone system inhibitor.

history, therapeutic procedures, and clinical events during the patient's hospital stay. The present study protocol complied with the Declaration of Helsinki and was approved by the institutional ethical committee of each participating institution. All study candidates were informed about data collection and blood sampling, and written informed consents were obtained.

A flowchart of patient selection is presented in Supplementary Figure 1. A total of 4,425 patients treated with ACEI at discharge, 2,158 with ARB, and 2,442 prescribed neither ACEI nor ARB (no RAS inhibitor) were enrolled in the present study. A direct comparison of survival benefit was performed between patients treated with ACEI and those with ARB at discharge. For the inverse probability of treatment weighting (IPTW) method using propensity score (PS), 5,563 eligible patients without missing data for Cox regression analysis were selected (3,784 and 1,779 patients with ACEI or ARB at discharge, respectively). For PS-matched analysis, 3,268 patients (1,634 in each treatment group) were selected and analyzed.

The primary end point was all-cause death, and the secondary end points were heart failure hospitalization and nonfatal re-myocardial infarction. For patients discharged alive, follow-up clinical data were obtained for 5 years. Categorical variables were compared by chi-square tests, and continuous variables were compared by the Kruskal-Wallis test for 3-group comparison (ACEI, ARB, and no RAS inhibitor) and Wilcoxon rank sum test for 2-group comparison (ACEI and ARB). The annual trend in the prescription rate of ACEI or ARB was assessed by the Cochran-Armitage trend test (Supplementary Figure 2). The Kaplan-Meier method was used to estimate event rates, and the differences were assessed by the log-rank test. Landmark analysis of the primary end point was also performed 2 years after survival discharge. Specifically, survival estimates were calculated in patients without any adverse events 2 years after survival discharge, because the Kaplan-Meier survival estimates for the ACEI and ARB treatment groups appeared to differentiate at this time point (Figure 1).

Inter- and intra-class drug differences in survival benefit were compared by age and sex-adjusted Cox regression analyses, and the hazard ratio (HR) and 95% confidence intervals (CI) were calculated using data obtained from the 2,442 patients without RAS inhibitors as a reference (Supplementary Figure 1). To reduce potential confounding effects due to patient background variability in the direct comparison between ACEI and ARB, the PS method was used in combination with Cox regression modeling. PS was defined as the probability of treatment assignment conditional on the measured baseline covariates. The inverse probability of treatment weighting method based on the PS was used to reduce confounding in time-to-event observational data.[16] To confirm the robustness of the inverse probability of treatment weighting results, we also performed PS matching with a caliper width of 0.001.[16] For the estimation of PS, we used a logistic regression model in which the treatment status (ACEI or ARB) was regressed on the following baseline characteristics: age, gender, body mass index, diabetes, hypertension, dyslipidemia, smoking, previous myocardial infarction, ST elevation myocardial infarction, Killip's classification, reperfusion therapy, and prescription of β blockers, calcium channel blockers, statins, diuretics, and antiplatelet agents.

Table 1
Demographics and clinical characteristics of the study population by treatment group

Parameter	No RASI (n = 2442)	ACEI (n = 4425)	ARB (n = 2158)	p-Value (Total)	p-Value (ACEI vs ARB)
Age (years)	67 (59–75)	65 (57–73)	67 (59–75)	<0.001	<0.001
Men	73.6%	77.9%	74.3%	<0.001	0.001
Body mass index (kg/m^2)	23.0 (21.0–25.2)	23.5 (21.5–25.7)	23.9 (21.6–26.0)	<0.001	0.001
ST-elevation myocardial infarction	82.3%	86.8%	83.7%	<0.001	<0.001
Diabetes mellitus	34.7%	32.6%	34.0%	0.19	0.27
Hypertension	49.4%	59.3%	70.3%	<0.001	<0.001
Dyslipidemia	40.6%	44.8%	46.5%	<0.001	0.19
Smoking	59.3%	66.0%	61.5%	<0.001	<0.001
Previous myocardial infarction	13.6%	11.9%	10.8%	0.02	0.18
KILLIP class				<0.001	0.01
1	79.5%	85.4%	84.2%		
2	9.1%	8.4%	7.4%		
3	4.1%	3.3%	4.4%		
4	7.3%	2.9%	4.0%		
Emergent coronary angiography	92.7%	95.3%	96.2%	<0.001	0.10
Target Lesion				<0.001	0.22
Left main	3.1%	0.9%	1.3%		
Left anterior descending artery	38.6%	47.9%	46.2%		
Right coronary artery	38.7%	34.9%	34.2%		
Left circumflex artery	16.3%	12.9%	14.8%		
Diagonal branch	3.0%	3.2%	3.4%		
Graft	0.4%	0.1%	0.1%		
Reperfusion therapy					
Percutaneous coronary intervention	80.4%	89.8%	93.2%	<0.001	<0.001
Thrombolysis	8.2%	7.1%	6.6%	0.12	0.49
Coronary artery bypass graft	6.6%	0.9%	1.4%	<0.001	0.07
Hemoglobin A1c (%)	6.0 (5.56.9)	5.9 (5.5–6.9)	6.0 (5.6–7.0)	0.01	0.001
Total cholesterol (mg/dL)	187 (158–218)	190 (164–220)	193 (166–224)	<0.001	0.02
Low-density lipoprotein cholesterol (mg/dL)	113 (87–139)	122 (99–148)	124 (101–149)	<0.001	0.57
High-density lipoprotein cholesterol (mg/dL)	45 (37–53)	44 (38–53)	44 (37–52)	0.78	0.49
Triglyceride (mg/dL)	91 (60–137)	94 (60–143)	99 (64–149)	<0.001	0.002
Estimated glomerular filtration rate (mL/min/1.73 m^2)	47.9 (33.8–61.8)	51.8 (41.2–64.5)	52.8 (40.9–65.4)	<0.001	0.35
Peak creatine phosphokinase (IU/L)	1701 (793–3400)	2025 (925–3801)	1793 (910–3503)	<0.001	0.02
Echocardiography data					
Left ventricular end-diastolic dimension (mm)	50.0 (46.0–54.0)	50.0 (46.5–54.0)	50.9 (47.0–55.0)	0.04	0.03
Left ventricular end-systolic dimension (mm)	34.0 (30.0–40.0)	34.0 (30.0–39.0)	34.0 (30.0–39.0)	0.051	0.04
Left ventricular ejection fraction (%)	52.6 (43.8–60.3)	53.5 (44.6–60.7)	55.6 (46.3–62.2)	<0.001	<0.001
Medication at discharge					
Beta-blocker	35.5%	48.8%	62.9%	<0.001	<0.001
Calcium channel blocker	26.0%	18.6%	19.7%	<0.001	0.27
Statin	29.7%	39.6%	57.0%	<0.001	<0.001
Antiplatelet	91.0%	98.1%	98.5%	<0.001	0.35
Diuretic	30.7%	26.9%	26.5%	<0.001	0.74
Follow-up duration (days)	1416 (345–1792)	1635 (707–1798)	1032 (343–1737)	<0.001	<0.001

Categorical variables are presented as number (percentage), and continuous variables are presented as the median (25-75 percentiles). Laboratory data were measured on admission.

Statistical significance was set as $p < 0.05$. All statistical analyses were performed using SAS, version 9.3 (SAS Institute Inc., Cary, North Carolina), or R software packages, version 2.15.1 (R Development Core Team, Vienna, Austria).

The corresponding author had full access to all the data in the study and took responsibility for the integrity of the data and the accuracy of the data analysis.

Results

Patient characteristics based on treatment group are summarized in Table 1. Significant differences in nearly all background variables were detected among the ACEI, ARB, and no RAS inhibitor treatment groups. Notably, patients in the no RAS inhibitor group were less frequently treated with evidence-based medications. Between the ACEI and ARB treatment groups, patients who received ACEI had lower prescription rates for state-of-the-art medications at discharge, such as β blockers and statins, partly because these patients were likely registered in the earlier period of the OACIS registry (Supplementary Figure 2). In the PS-matched cohort, patient characteristics were well balanced (Supplementary Table 1).

Annual trends in the prescription rate of RAS inhibitors are shown in Supplementary Figure 2. The prescription rate

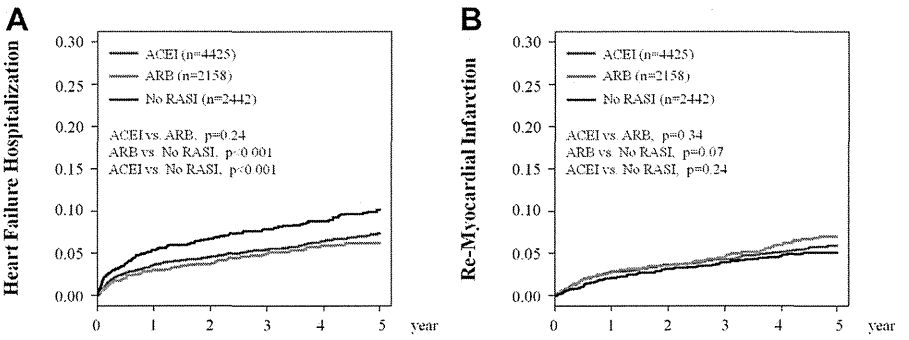

Figure 2. Cumulative event rates of heart failure hospitalization *(A)* and nonfatal re-myocardial infarction *(B)* in the 3 treatment groups during a 5-year follow-up period. RASI = renin-angiotensin-aldosterone system inhibitor.

of ARB had increased annually until 2007, whereas that of ACEI decreased. In 2010, approximately 80% of all study patients received RAS inhibitors at discharge. The types of ACEI and ARB prescribed at discharge are listed in Supplementary Table 2.

A total of 661 deaths (no RAS inhibitor, 231; ACEI, 293; and ARB, 137), 512 heart failure hospitalizations (no RAS inhibitor, 174; ACEI, 250; and ARB, 88), and 375 nonfatal re-myocardial infarctions (no RAS inhibitor, 85; ACEI, 200; and ARB, 90) were recorded during a median follow-up period of 3.9 years (median 1,426 days, interquartile range 402 to 1,794). Kaplan-Meier survival analysis demonstrated that both the ACEI and ARB groups had better 5-year mortality than the no RAS inhibitor group (Figure 1). Age and sex-adjusted Cox regression analysis revealed that both ACEI and ARB treatments were associated with reduced 5-year mortality compared with no RAS inhibitor treatment (adjusted HR 0.70, 95% CI 0.58 to 0.83, $p < 0.001$ for ACEI and adjusted HR 0.79, 95% CI 0.64 to 0.98, $p = 0.03$ for ARB, respectively). However, treatment with ACEI was associated with significantly lower 5-year mortality compared with that with ARB (Figure 1). Landmark analysis demonstrated that the superiority of ACEI with regard to long-term prognostic impact was only evident after 2 years of discharge. In addition, the survival estimate of the ARB group from 2 to 5 years after survival discharge was comparable to that of the no RAS inhibitor group (Figure 1). These observations were consistent with those obtained in the PS-matched cohort (Figure 1). In contrast to the survival rates, no significant differences in heart failure hospitalization or nonfatal re-myocardial infarction rates were detected between the ACEI and ARB groups (Figure 2).

Cox regression analysis in the PS-weighted sample revealed that the adjusted HRs of 2-year mortality in the ACEI group compared with the ARB group was 1.05 (95% CI 0.76 to 1.47, $p = 0.76$) in the first 2 years after survival discharge and 0.53 (95% CI 0.38 to 0.74, $p < 0.001$) from 2 to 5 years after survival discharge (Figure 3). These results are consistent with those obtained by the Cox regression analyses in the PS-matched sample. The adjusted HR of 2-year mortality was 1.17 (95% CI 0.77 to 1.76, $p = 0.46$) in the first 2 years after survival discharge and 0.56 (95% CI 0.34 to 0.91, $p = 0.02$) from 2 to 5 years (Figure 3). Subgroup analysis suggested that ACEI and ARB had generally comparable prognostic impacts for the 2 years after discharge, with the exception of the subgroups without hypertension (Figure 3), and that ACEI was associated with better survival from 2 to 5 years after discharge, except in patients aged ≤60 years (Figure 3). Intraclass drug comparisons revealed that both ACEI and ARB displayed similar effectiveness compared with the no RAS inhibitor patient group in the first 2 years after survival discharge (Figure 4). However, treatment with ACEI, but not with ARB, was associated with better mortality rates from 2 to 5 years after survival discharge in comparison with the no RAS inhibitor treatment group (Figure 4).

Discussion

We compared the long-term prognostic impacts of ACEI and ARB after AMI using a multicenter prospective observational registry database in Japan. The results primarily showed that treatment with either ACEI or ARB was associated with better 5-year survival compared with patients who did not receive either drug, confirming the clinical importance of RAS inhibition in post-AMI patients. However, our results further demonstrated that patients treated with ACEI had significantly lower long-term mortality compared with those treated with ARB from 2 to 5 years after AMI with the comparable prognostic impacts between ACEI and ARB in the first 2 years.

The present study is the first to compare the long-term prognostic impacts of ACEI and ARB in post-AMI patients in the contemporary percutaneous coronary intervention (PCI) era. The observation that prognostic impacts in the first 2 years after discharge of AMI were comparable between ACEI and ARB was consistent with the results derived from the OPTIMAAL and VALIANT RCTs,[6,7] which demonstrated comparable benefits between ACEI and ARB in post-AMI patients with relatively short follow-up periods. In contrast, we also demonstrated the better prognostic impact of ACEI beginning after 2 years of AMI onset, which was partly consistent with findings reported by Savarese et al.[17] In a meta-analysis of 26 RCTs comparing ACEI or ARB versus placebo in 108,212 patients at high cardiovascular risk without heart failure, they revealed that only ACEI, but not ARB, reduced the risk of all-cause death, whereas ACEI and ARB both reduced the risk of the composite outcome of cardiovascular death, myocardial infarction, and stroke.[17] We speculate that the mechanism for the superiority of ACEI over ARB treatment may be explained by a reduction in angiotensin II production and activation of the kallikrein-bradykinin system with ACEI treatment or prolonged elevation of angiotensin II levels